Journal of Sedimentary Research

Journal of Sedimentary Research, 2021, v. 91, 751–772
Research Article
DOI: 10.2110/jsr.2020.174

LATERALLY ACCRETED DEPOSITS IN LOW EFFICIENCY TURBIDITES ASSOCIATED WITH A STRUCTURALLY-INDUCED TOPOGRAPHY (OLIGOCENE MOLARE GROUP, TERTIARY PIEDMONT BASIN, NW ITALY)

ROBERTO TINTERRI AND ANDREA CIVA*
Department of Chemistry, Life Sciences and Environmental Sustainability, Earth Sciences Unit, University of Parma, Italy
e-mail: roberto.tinterri@unipr.it

ABSTRACT: **The origin of laterally accreted deposits in ancient deep marine successions is often controversial. Indeed, not always do these features imply the occurrence of meanders or high-sinuosity turbidite channels, but they can be generated by other causes, such as sediment-gravity-flow dynamics controlled by the morphology of tectonically confined mini-basins. This work discusses laterally accreted deposits composed of sharp-based, normally graded beds in a very small tectonically controlled mini-basin. These beds, characterized by a well-defined asymmetrical cross-current facies tract, form well-developed lateral-accretion surfaces dipping in directions ranging between W and SW, and perpendicular to the paleocurrents directed towards the N. For this reason, these deposits have always been interpreted as point bars related to meandering channels. A new detailed stratigraphic framework and facies analysis have led to an alternative interpretation, namely that these deposits record lateral deflections of small volume, longitudinally segregated turbidite dense flows against a structurally controlled morphological high. This interpretation is also supported by a comparison to other tectonically controlled turbidite systems that are characterized by higher degrees of efficiency but show similar laterally accreted deposits and cross-current facies tracts.**

INTRODUCTION

This work discusses laterally accreted deposits, generated by small-volume and sand-rich sediment gravity flows in the small tectonically confined Mioglia mini-basin. This mini-basin is located in the western part of the Tertiary Piedmont Basin (TPB) in NW Italy, which is a large polyhistoric episutural basin that has many similarities with ponded basins in slope settings (Fig. 1) (Mutti et al. 2002).

Laterally accreted deposits in deep-water environments are common depositional elements of modern fans that are, generally, fed by mud-rich terrigenous sediment sources and are usually associated with meandering belts (e.g., Abreu et al. 2003; Mutti et al. 2003; Wynn et al. 2007; Kolla et al. 2007; Dykstra and Kneller 2009 and Janocko et al. 2013). Nevertheless, the nature and origin of the laterally accreted deposits in ancient deep marine successions are often controversial (e.g., Mayall et al. 2006; Maier et al. 2012, 2013; Pickering and Hiscott 2016). Indeed, these types of features do not always imply the existence of meandering or high-sinuosity turbidite channels since they can be generated by other causes (e.g., Labourdette and Bez 2010; Gamberi and Marani 2011; Gamberi et al. 2013; Maier et al. 2012, 2013; Pickering and Hiscott 2016; Edwards et al. 2017).

From this point of view, this work is intended to show how laterally accreted deposits can be related to lateral deflection of small-volume sediment gravity flows against a structural high, and how these types of deposits can be related to the interaction between the dynamics of sediment gravity flows and the complex morphology of tectonically confined mini-basins. A correct interpretation of these controversial deposits is fundamental not only from a basin analysis standpoint but also for oil exploration, since, in these types of basins, they can form important hydrocarbon reservoirs (e.g., Prather et al. 1998; Abreu et al. 2003; Mutti et al. 2003). For this purpose, an appropriate interpretation can be achieved only through accurate integration between detailed sedimentological data and profound knowledge of the geological setting.

In the Mioglia basin, the occurrence of inclined graded beds associated with right-angle paleocurrent directions has always led these deposits to be interpreted as deep-sea point bars related to meandering channels. In particular, one of these sandstone bodies has become famous due to the description by Mutti and Normark (1991) (see their Figure 4.11; see also Mutti et al. 2002). However, detailed stratigraphic framework and facies analysis have highlighted new evidence that suggests a possible alternative interpretation. These deposits are indeed characterized by an asymmetrical coarse-grained cross-current facies distribution, very similar to that of other tectonically confined turbidite systems, which can be interpreted as related to flow deflections against a pronounced tectonically controlled confining slope of the basin (see Tinterri et al. 2017; Cunha et al. 2017). In particular, the characteristics of these cross-current facies tracts, induced by flow deflections, are thought to change in accordance with the relationship between the degree of efficiency of the turbidite system (*sensu* Mutti et al. 1999) and the degree of basin confinement, where the efficiency can be seen as the ability of the flow to carry its sediment load basinward and to segregate its grain-size populations into well-developed and distinct facies over distance. All things being equal, this ability can depend on the

* Present Address: Eni S.p.A., via Emilia 1, San Donato Milanese, Milano, Italy

Published Online: July 2021
 1527-1404/21/091-751

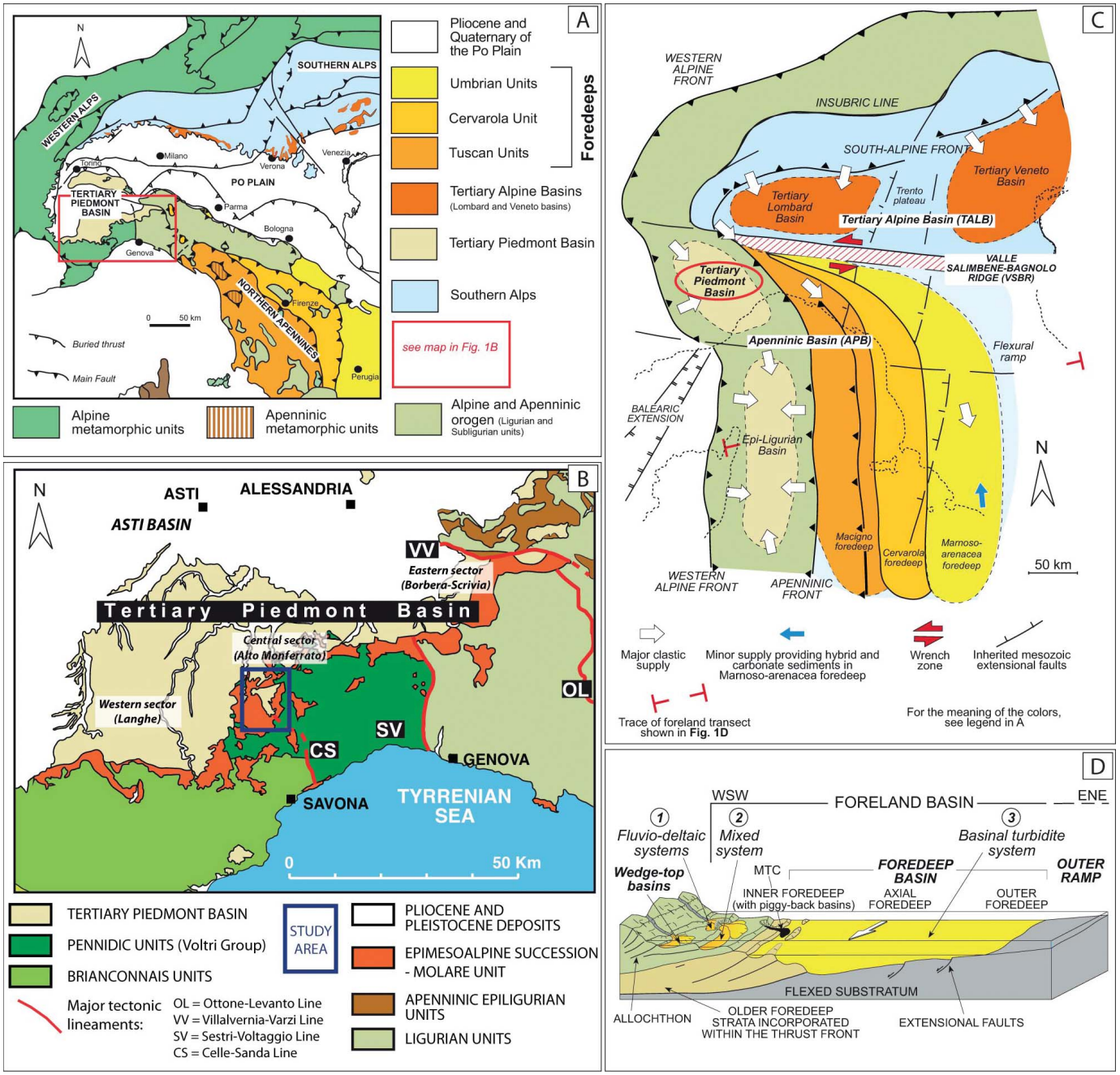

FIG. 1.—**A)** A simplified geological map of northern Italy showing the main tectonic and depositional elements (from di Biase and Mutti 2002). In the red square, the area shown in Part B. **B)** Simplified geological map of the junction between the Alps and the Apennines showing the Tertiary Piedmont basin (from Mutti et al. 2002). In the blue square, the study area shown in Figure 2A. **C)** Physiographic map depicting the inferred configuration and main features of the Proto-Adriatic Basin from late Oligocene to middle Miocene (from di Biase and Mutti 2002). **D)** Diagram showing the main elements of a foreland basin and the relationships between a growing orogenic wedge and the outer flexed board (from Mutti et al. 2003).

geometry and the degree of basin confinement, which can favor decelerations hindering flow evolution (Tinterri et al. 2016, 2017). From this point of view, this work presents a case of very low efficiency in very small turbidite basins, less than 1 km across (see type D basin by Mutti and Normark 1987; see also Cazzola et al. 1981).

Consequently, the main objectives of this work are: 1) to describe the relationship between the cross-currents facies tract and the tectonically controlled morphology of the basin through detailed physical stratigraphy and facies analysis, and 2) to discuss an alternative hypothesis to the point bar, based on the possibility that the deflection of sediment gravity flows produced by tectonically controlled morphology has played a fundamental role, and 3) to compare this example to other confined basins and develop a conceptual model of cross-current facies tract variations related to flow efficiency.

GEOLOGICAL AND STRATIGRAPHIC SETTING

This study focuses on a small sand-rich turbidite system (the Fraschetto turbidite system) in the Molare Group, a Rupelian succession cropping out in the western sector of the Tertiary Piedmont Basin (TPB), (see Fig. 1A, B).

This basin is a long-lived polyhistoric episutural basin (from late Eocene to Messinian) deposited after the Mesoalpine collisional event between the European and Adria plates (Fig. 1C, D; Elter and Marroni 1991; Mutti et al. 1995; Maino et al. 2013; Molli et al. 2010). Consequently, the Molare Group records a complex geodynamic setting represented by the Western Alps–Northern Apennines junction area, i.e., the Ligurian Knot (Laubscher 1991; Laubscher et al. 1992). In this area, several deformative phases and basin inversions, mainly related to extensional and transtensional fault systems, controlled deposition (e.g., Falletti et al. 1995; Mutti et al. 1995, 2002; Rossi et al. 2009; Maino et al. 2013; Ghibaudo et al. 2014). Specifically, the Molare Group was deposited in the Tertiary Epimesoalpine Basin, which predates the late Oligocene and Neogene foredeeps of the northern Apennines (Mutti et al. 1995).

The Molare Group forms the basal part of the TPB succession and records an overall transgressive event that unconformably overlies an Alpine substratum deformed during the Mesoalpine collisional events (Lorenz 1969; Mutti et al. 1995; Gelati and Gnaccolini 2003). The basal part of the Molare succession is characterized by conglomerate and pebbly-sandstone facies that can be interpreted as alluvial-fan and fan-delta deposits in a basin strongly controlled by extensional faults with mainly NNW direction. Many of these faults remained active during the sedimentation of the Molare Group, undergoing progressive inversion over time (Fig. 2A, C; see Mutti et al. 1995, 2002).

The overall deepening-upward succession of the Molare Group can be subdivided into three smaller-scale unconformity-bounded units or allogroups (see M1, M2, and M3 in Fig. 2B), each of which is characterized by a forestepping–backstepping wedge of clastic facies produced by a regressive–transgressive cycle (Mutti et al. 2002). Each allogroup records an initial abrupt forestepping of coarse-grained strata followed by a gradual backstepping of these deposits passing upward into a mudstone-dominated succession. An allogroup is thought to result from a phase of structural deformation and related uplift followed by a period of relative tectonic quiescence and subsidence; in tectonically active basins, they record the main stages of the basin paleogeographic evolution as related to successive phases of tectonic deformation (Mutti et al. 2002).

In the study area, the M1 allogroup consists of a basal member representing flood-dominated alluvial-fan and fan-delta systems, mainly composed of conglomerate and pebbly-sandstone facies (Mutti et al. 2002; Ghibaudo et al. 2014). These sediments were deposited in a series of small sub-basins controlled by high-angle normal faults rooted in the pre-Oligocene substratum and were fed by local basement highs through flood-dominated stream flows (see Units "a" and "b" in Fig. 2C). These normal faults control the subsidence-driven transgression and the paleocurrents of the fluvio-deltaic systems, which, in the Mioglia area, are directed toward the SW (Mutti et al. 1995, see also Tinterri 1994). This transgression led to widespread deposition of a middle sandy member predominantly consisting of fossiliferous flood-generated delta-front sandstone lobes (Units "c" and "b" in Fig. 2A, C) that grade upward into open marine and generally highly fossiliferous prodelta siltstones and mudstones recording a phase of basin deepening and starvation (Unit "e" in Fig. 2A, C).

Unit M2 sharply overlies the mudstone of unit M1 and consists of highly laterally discontinuous, small coarse-grained sand-rich turbidite systems, which are the object of this study. These small turbidite systems are characterized by lenticular units of conglomerates and amalgamated sandstones with pronounced basal erosional surfaces (e.g., the Fraschetto and Valla systems, see Fig. 2A, C; Mutti et al. 1995). The composition of M2 strata, which grade upward into mudstone-dominated deposits, is similar to that of the underlying M1 conglomerates and fossiliferous sandstones. Consequently, M2 sandstone units can be related to the resedimentation of M1 Molare strata in adjacent structurally confined depressions. This process occurred along fault-controlled basin margins characterized by reverse faults related to the reactivation of pre-existing high-angle normal faults. In particular, in the Mioglia basin, these fault-controlled basin margins are related to two different fault systems. One system consists of WSW–ENE-oriented transtensional faults accommodating left-lateral displacements and is represented by the Merana–M. Acuto system in the northern part of the basin (see Fig. 2A). The other one consists of NNW–SSE-oriented faults that record a right-lateral transpression represented by the Mioglia flexure, located to the SW, and the Garbarini fault, as well as other minor parallel faults with the same orientation, located 4 km to the NE (Fig. 2; Bernini and Zecca 1990; see also Rossi and Craig 2016). Movements along these reverse faults could produce the collapse of the underlying Molare 1 strata forming extremely poorly organized and highly immature gravity-flow deposits (e.g., the Valla and Fraschetto turbidite systems; see Cazzola and Rigazio 1983; Mutti et al. 1995, 2002).

Finally, unit M3 consists of relatively thick and cyclically stacked low-efficiency turbidite systems (e.g., the Mioglia system by Cazzola and Rigazio 1983; see Fig. 2A, B) abruptly resting on and locally cutting into the fine-grained deposits of the underlying M2 unit.

METHODOLOGY

This study is based on detailed facies analysis and bed-by-bed measurement of 37 stratigraphic logs for a total thickness of about 700 m (see Figs. 3, 4; see also Civa 2013 and Tinterri and Civa 2014). More precisely, the framework of the seven turbidite units with lateral accretions has been developed based on a general stratigraphic cross section (Fig. 4). Moreover, five cross sections resulting from closely spaced, detailed logs have been reconstructed to highlight the lateral facies variations of these seven units.

The sandstone units with lateral-accretion surfaces were followed in the field and were mapped (see Fig. 3). This mapping has been fundamental to guide the stratigraphic correlations shown in the stratigraphic cross section of Figure 4. However, these correlations have also been achieved by correlating first the principal key beds, represented by the condensed section at the top of unit "d" of Molare 1, and then the seven sandstone units that can be traced over the entire study area (see Figs. 2C, 3, 4).

These high-resolution correlations have been used to identify the facies tract of the beds characterizing the laterally accreted deposits. The concepts of a bed, deposited by one event, and of bedsets characterizing the Fraschetto sandstone units come from Campbell (1967), (see below, Figs. 5 and 6). In the same way, a facies tract can be defined as the facies observed within the same bed or within the same bedset, as described by Campbell (1967), along an ideally synchronous depositional profile reconstructed through detailed stratigraphic correlations and paleocurrent directions (Lowe 1982; Mutti 1992; Mutti et al. 1999). Consequently, these facies represent the deposit of the same flow or similar flows undergoing transformations along its (or their) down-slope motion. Specifically, the general reference facies scheme used in this work is that by Mutti et al. (2003) (see their Figs. 13, 14), which introduced seven facies types (F2 to F9) describing the down-current evolution of a waning and depletive turbidity current.

However, this work is also based on the facies scheme and interpretations presented by Tinterri et al. (2017), which discussed the sedimentary characteristics of cross-current facies tracts related to flow modifications induced by asymmetrical structurally controlled basin morphology (see their Fig. 15). In particular, these authors have shown that structurally confined foredeeps are characterized by well-determined facies associations related to flow decelerations induced by basin

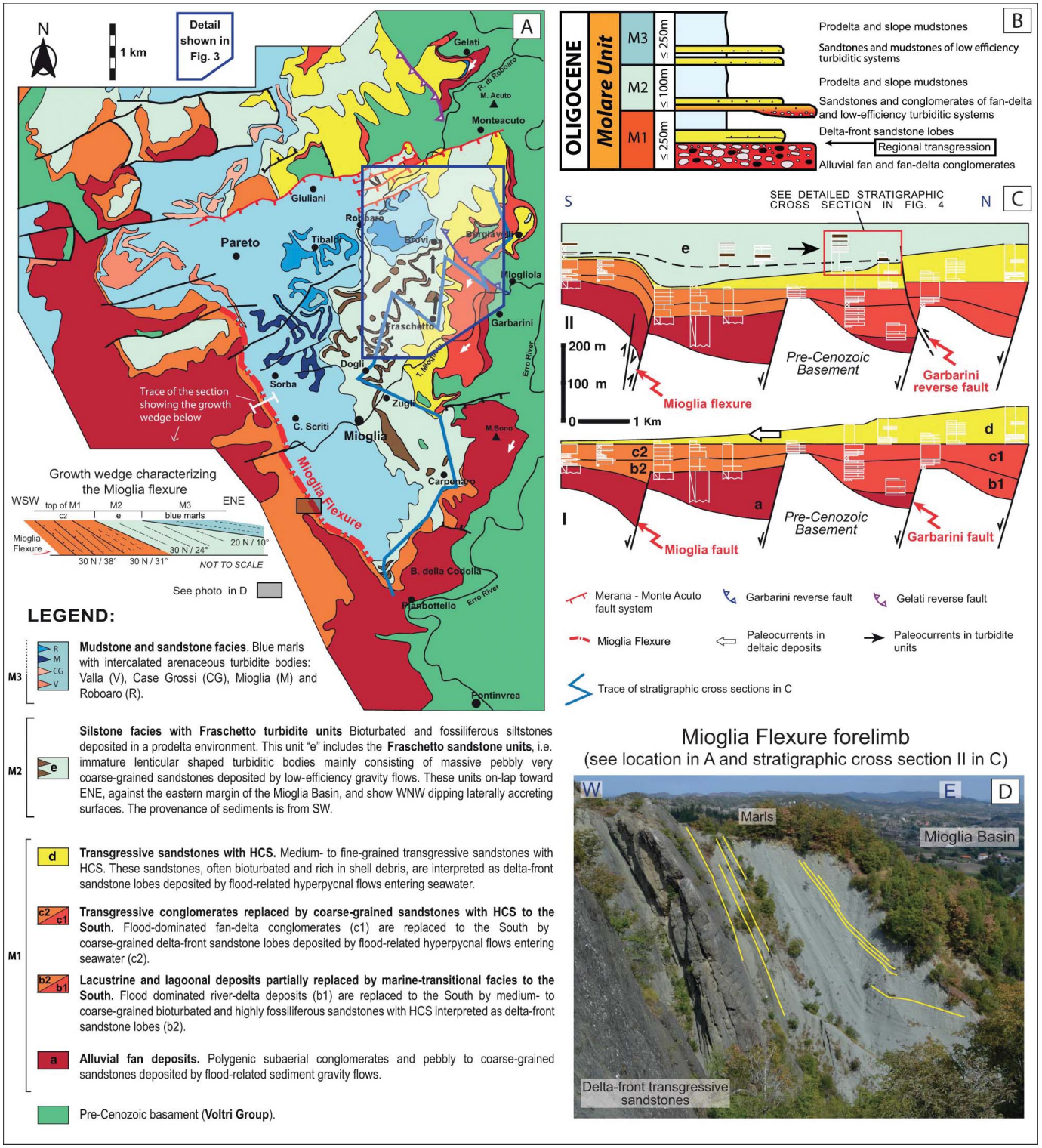

FIG. 2.—**A)** Geological map of the Mioglia basin showing the relationships between allogroups Molare 1, 2, and 3 depicted in Part B (modified from Mutti et al. 1995; see also Bernini and Zecca 1990). On the left, the growth wedge that can be observed perpendicular to the Mioglia flexure is also shown. It should be noted that this implies a synsedimentary tectonic inversion of this structure particularly evident during the M2 group deposition. **B)** Deepening-upward succession of the Molare Group subdivided into three smaller-scale unconformity-bounded units or allogroups (M1, M2, and M3, Mutti et al. 2002). **C)** Stratigraphic cross section of the M1 and M2 allogroups in the Mioglia area (see Part A for the location of the cross-section trace). The lower part of succession "I" is recorded by the M1 Unit, consisting of alluvial-fan deposits and transgressive fan-delta strata characterized by north-derived flood-dominated gravity flows. The upper part of the stratigraphic cross section "II" consists of mudstone facies recording the tectonically controlled basin deepening associated with a tectonic inversion that produced the resedimentation of the M1 deposits into the adjacent basin by south-derived gravity flows (modified from Mutti et al. 1995). **D)** Delta-front sandstone lobes of the M1 group consisting of massive pebbly very coarse-grained sandstones verticalized along the Mioglia flexure in the southern part of the basin (see Part A for the location of the outcrop).

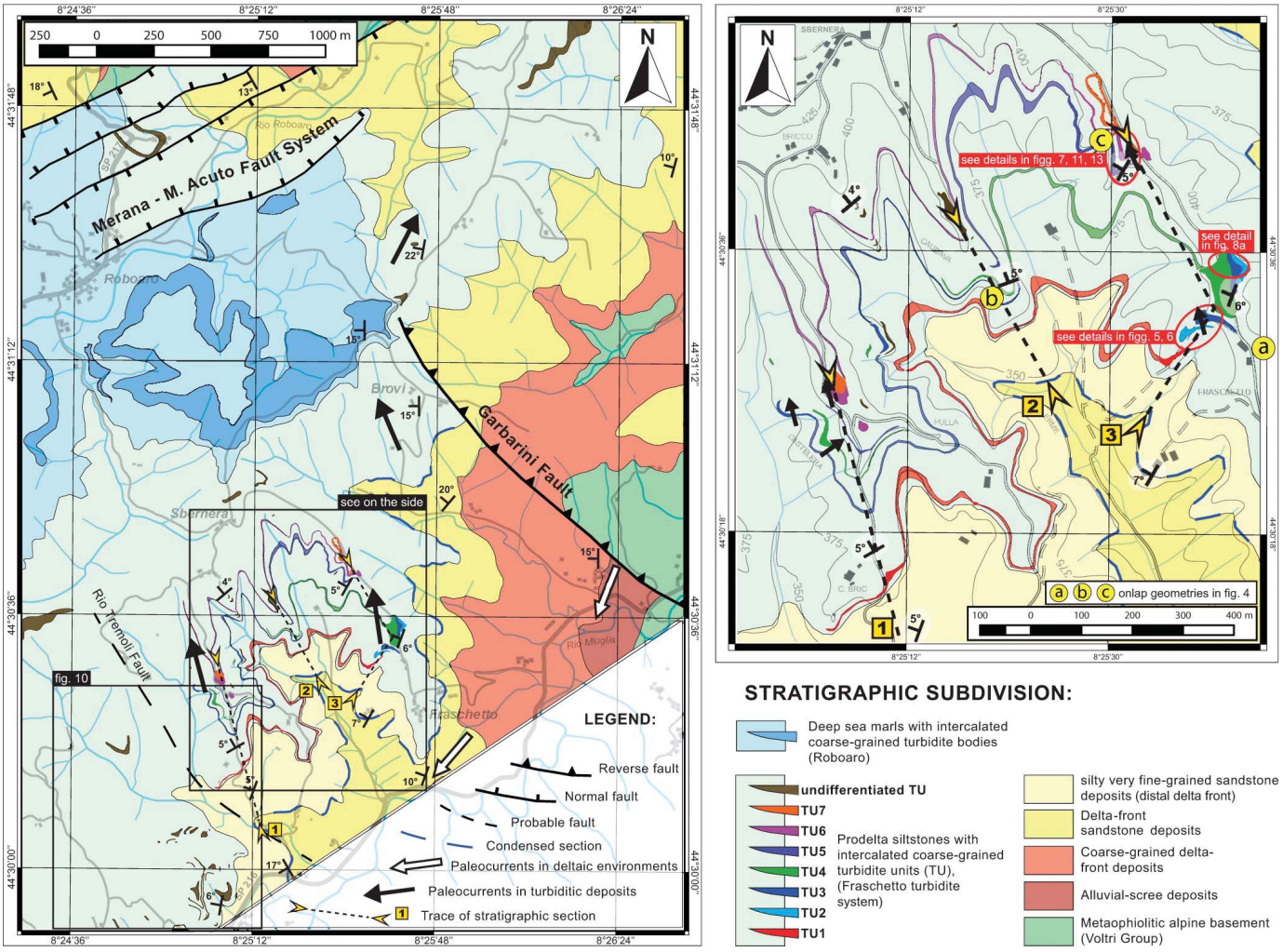

FIG. 3.—Geological maps showing the closure of the Fraschetto turbidite units against the Garbarini structural high (see Fig. 2A for the map location and a description of the stratigraphic units).

confinement (see also Tinterri and Muzzi Magalhaes 2011; Tinterri and Tagliaferri 2015; Tinterri et al. 2016; Cunha et al. 2017).

THE FRASCHETTO TURBIDITE SYSTEM IN THE STRUCTURALLY CONFINED MIOGLIA BASIN

Introduction: Stratigraphic Framework

The detailed field mapping and high-resolution physical stratigraphy performed in this work in the area around the Garbarini fault (see Figs. 3, 4) show that the Fraschetto turbidite system is characterized by seven main sand-rich turbidite units that are well developed to the southwest of the fault but disappear to the northeast of this structure (see Figs. 3, 4). The general stratigraphic cross section (Fig. 4) shows also an evident stratigraphic pinch-out of the upper Molare succession toward NE, i.e., against the Garbarini fault, where the laterally accreted sandstone units of the Fraschetto system are characterized by onlap relationships (see Fig. 5, where the closure of basal Units 1, 2, and 3 can be observed; see also Fig. 4). Furthermore, angular unconformities and stratigraphic pinch-outs towards the E and NE can be recognized at various scales in the studied stratigraphic succession (see Fig. 4), highlighted also by a progressive upward decrease in dip magnitude of the turbidite units (their basal and uppermost surfaces) in the Fraschetto area. These growth wedge structures can be also observed along the Mioglia flexure between the upper part of the M1 and M2 units (see Fig. 2A), suggesting, as better explained below, that an important synsedimentary activity occurred during the deposition of Fraschetto turbidite system. Thus, the Fraschetto sand-rich turbidite units are clearly related to the synsedimentary activity of the Mioglia and Garbarini structures (see Figs. 2, 4).

The Sedimentary Characteristics of Laterally Accreted Sandstone Units

The seven main sand-rich turbidite units of the Fraschetto turbidite system are generally 2–6 m thick and 50–500 m wide and are composed of a series of sharp-based and normally graded beds that are about 0.5–2 m thick and 5–50 m wide. These beds are also rich in shallow-water fossils, such as bivalves and Gastropoda, and even trace fossils, such as *Ophiomorpha*, are very common, especially at the base of the turbidite units (see Fig. 4, 5D).

The sharp-based and normally graded beds that compose these large-scale lenticular turbidite units dip towards the WSW, as can be observed in

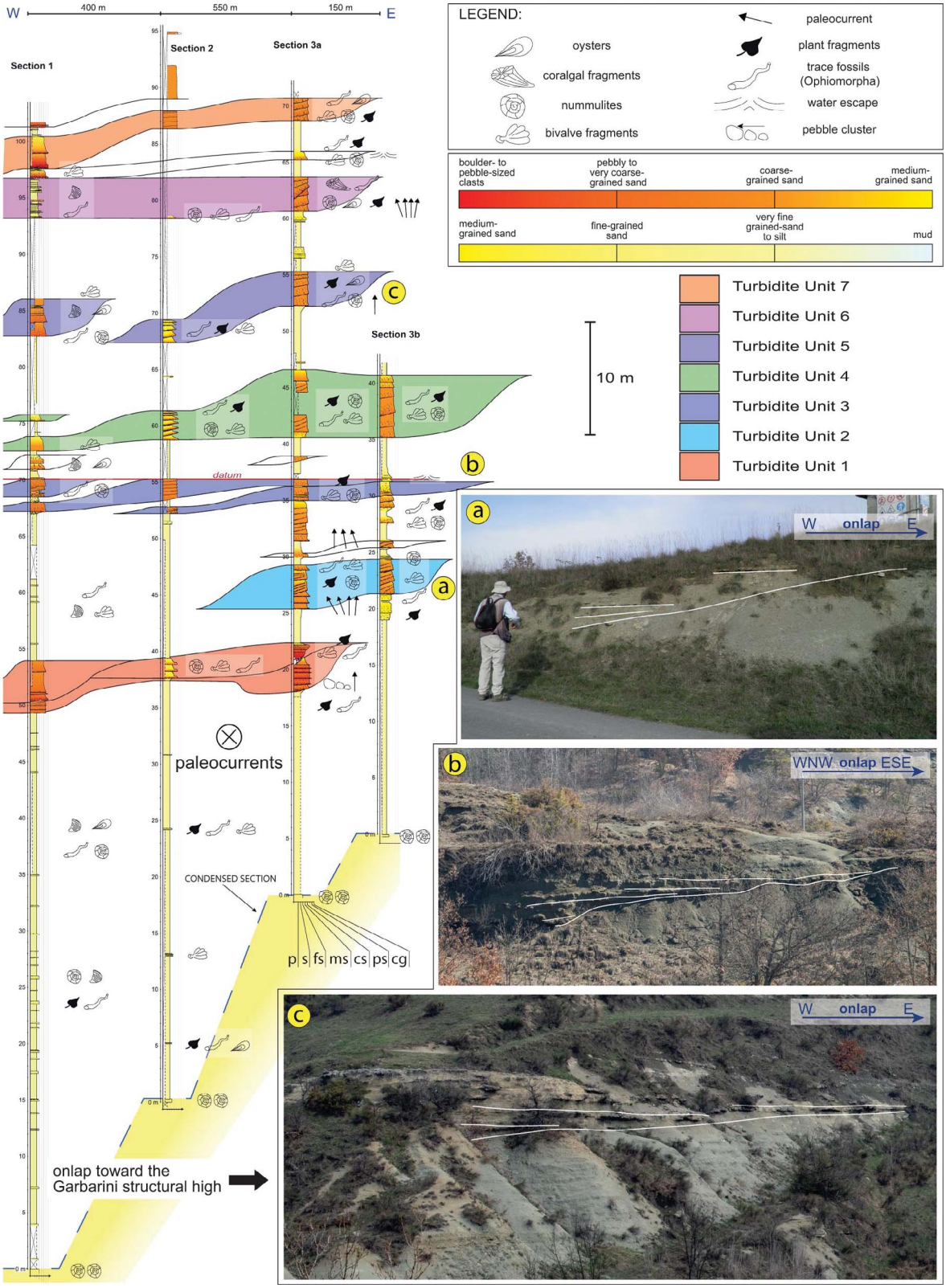

FIG. 4.—Detailed stratigraphic cross section illustrating the progressive pinching out of the Fraschetto turbidite units towards the Garbarini structural high (i.e., to the ENE), in a cross-current cut (see Fig. 2C for the location of the cross section). **A–C)** Stratigraphic unconformities and Fraschetto turbidite unit pinch-outs to the NE and ENE. In particular, panoramic views "B" and "C" show tabular sandstone lobes cropping out in the western zones of the study area (see logs 1 and 2). These lobes are laterally equivalent to the eastern turbidite units 3 and 5, respectively, which are characterized by laterally accreted deposits near the structural high.

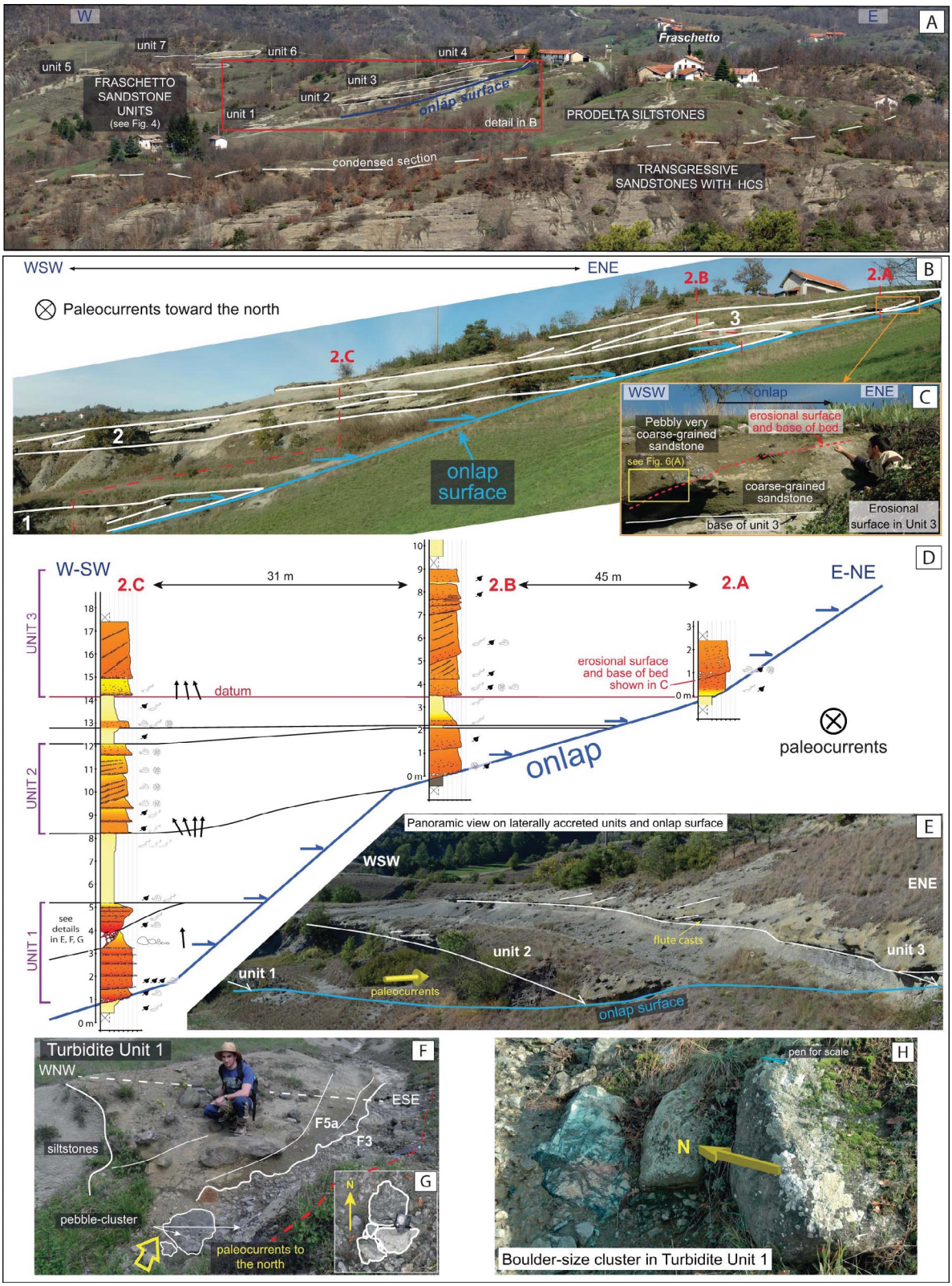

FIG. 5.—**A)** Panoramic view of the onlap of the basal Fraschetto sandstone units (M2) and the underlying transgressive fan delta (M1), in which the condensed section can also be observed (see map in Figure 3 for the location of the viewpoint). **B**, **C)** Panoramic views of the onlap in which laterally accreted beds dipping towards the WSW (i.e., perpendicular to the northward paleocurrents) can be observed. The photo detail in Part C shows the erosional surface dipping in the same direction of the laterally accreted deposits. **D)** Detailed stratigraphic cross section of the basal part of the Fraschetto turbidite system, in which the closure of the sandstone units 1, 2, and 3 against the onlap surface can be observed (see Figs. 3 and 4 for the location of the outcrop). **E)** Panoramic view of the onlap of units 1, 2 and 3. This is the same outcrop shown in Part B taken from another angle. **F)** Detail of the coarse-grained basal Unit 1; worth noting are the laterally accreted deposits dipping to the WNW and the boulder and cobble conglomerate is deposited towards the ESE (see Fig. 4A). **G**, **H)** Details of the basal orthoconglomerate showing cobble–pebble (Part G) and boulder (Part H) clusters indicating paleocurrents towards the north roughly parallel to the erosional surface (see dashed red line in Part F).

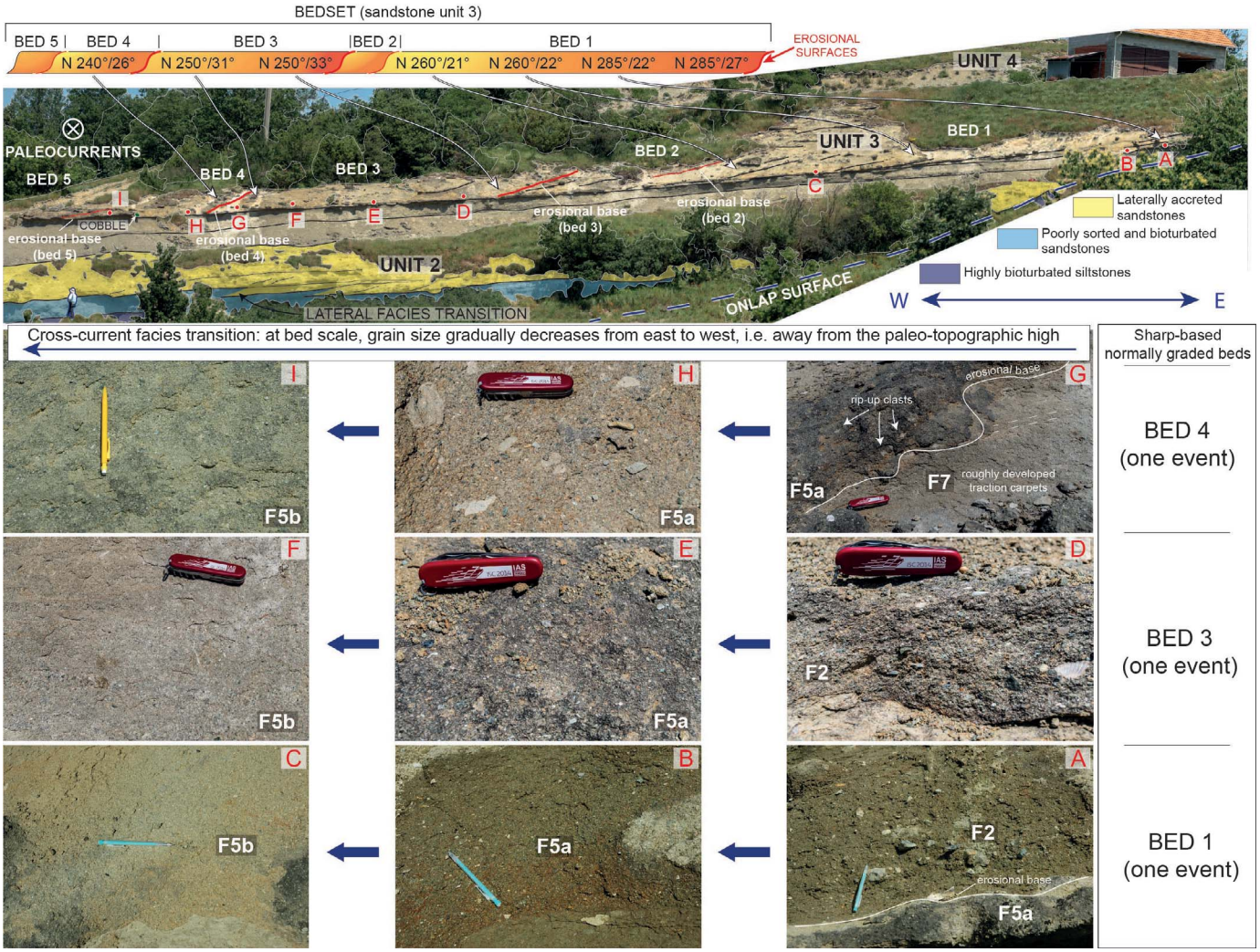

FIG. 6.—Details illustrating the large-scale sandstone Unit 3 composed of five sharp-based normally graded beds dipping to the WSW showing a decrease in grain size in the same direction. Below, details of these lateral grain-size changes characterizing beds 1, 2, and 3 are shown. The coarsest facies (F2) of bed 1 (see detail in A) is located towards the ENE and is characterized by the basal erosional surface dipping towards the WSW shown in the detail of Figure 5C.

the outcrops and diagrams of Figures 5–11. More precisely, each large-scale sandstone unit (2–6 m thick and 50–500 m wide) consists of the lateral juxtaposition of sharp-based and normally-graded beds (0.5–2 m thick and 5–50 m wide) and, in a cross-current direction, each inclined graded bed (deposited by one event) shows, from ENE to WSW, the following facies (see Figs. 12A, 13A, B): 1) pebble and cobble orthoconglomerates (F3 in the facies scheme by Mutti et al. 2003), where pebble, cobble, and boulder clusters (*sensu* Dal Cin 1968) indicate paleocurrents towards the north (see Fig. 5F, G, H); 2) very coarse sandy pebble paraconglomerates (F2) (Fig. 6A); 3) massive to crudely graded, poorly sorted very coarse-grained sandstones (F5a, Fig. 6B, E, H) that grade, over very short distances toward the WSW, into massive coarse-grained sandstones (F5b, Fig. 6C, F, I); 4) poorly developed, tabular massive to crude laminated coarse- to fine-grained sandstones (F5b, F8, F9), (see Figs. 4B, C, 13A, B). The coarsest-grained facies (F3, F2) are always concentrated to the ENE and are generally characterized by evident basal erosional surfaces that dip WSW, i.e., as do the lateral-accretion deposits (see Figs. 5F–H, 6A, 8). However, erosional bases can also be associated with F5a and F5b, as shown in Figures 7A, D, and 8. In particular, it is interesting to note that, in Unit 4, the laterally accreted deposits are closely associated with the high-angle erosional surface dipping to the WSW (see Fig. 8).

This evidence is considered very important, because the general dip of these laterally accreted deposits (in all the seven turbidite units in the entire study area) remains essentially constant, i.e., roughly towards the WSW and perpendicular to the NNW-oriented Garbarini structural high (see Figs. 5–10). These inclined bedding surfaces represent the bases of the beds (see Figs. 6, 7D) and the surfaces, within the beds, through which the facies changes occur (see below and Figs. 6, 7). In particular, the WSW-ward-dipping surfaces associated with the bases of the beds with sharp grain-size breaks are quite evident in Unit 3 (see Fig. 6). Nevertheless, analyzing the dip variations towards the WSW in detail, a slight change can be observed. In Unit 6, for example, if the strike direction, which can be considered roughly parallel to the paleocurrents, is taken into account, a rotation from NE (see the basal red erosional surface in Fig. 11) to the NW (see the bedding surfaces in Fig. 11) can be observed. A similar behavior also characterizes lower units 2 and 3, where the onlap surface can be very well observed (Fig. 5).

Each large-scale turbidite unit is bounded above and below by even, thin-bedded silty deposits, and scour marks at the bases of these sandstone units indicate paleocurrents directed toward the north, i.e., essentially

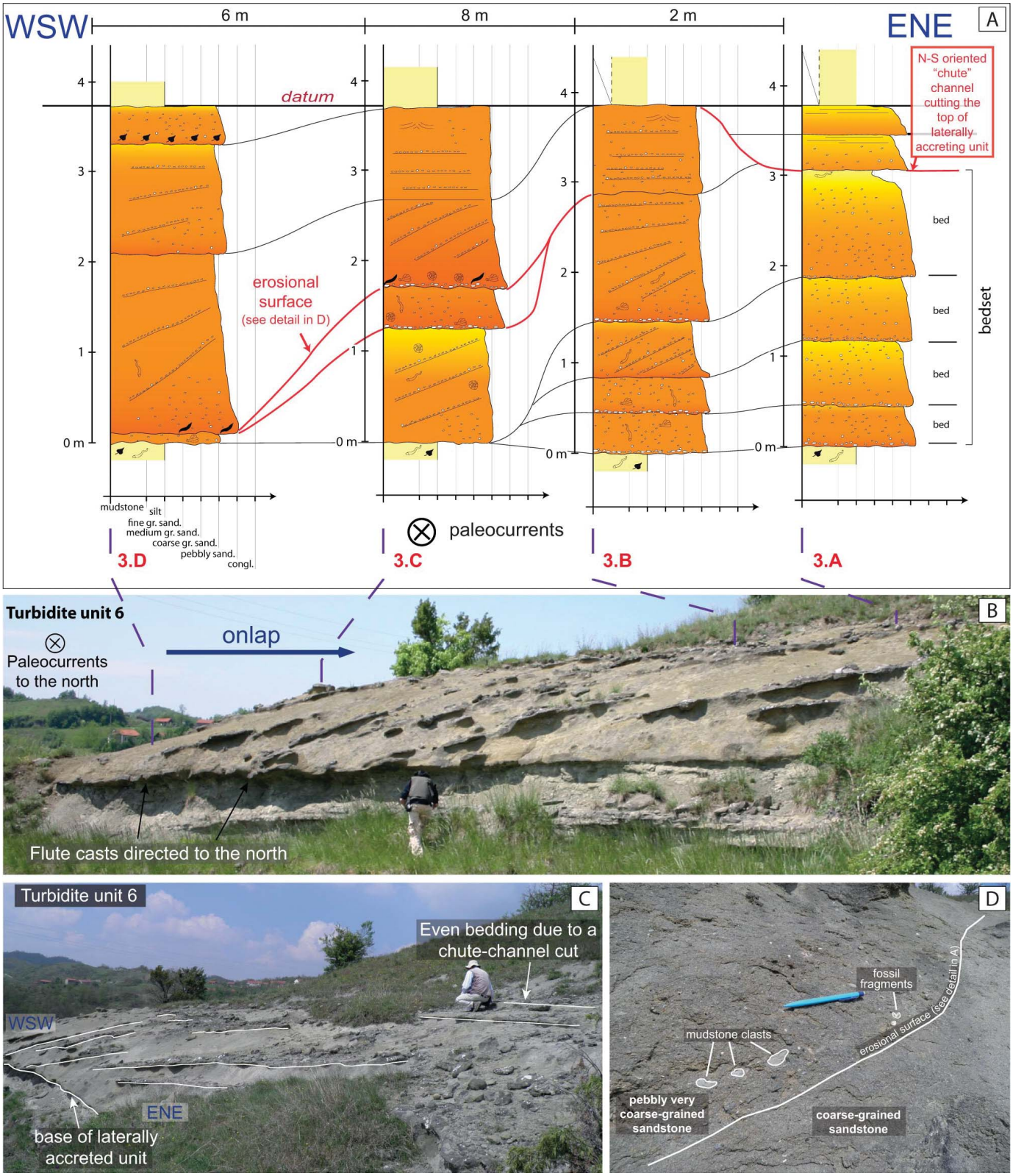

FIG. 7.—**A)** Detailed stratigraphic cross section of turbidite Unit 6, in which beds dipping to the WSW can be observed. **B)** Spectacular panoramic view of the laterally accreted deposits of Unit 6 (see Part A). **C)** Detail of Unit 6 from a different point of view highlighting the lateral accretions and horizontal bedding recording the deposition of a sort of "chute or cutoff." **D)** Detail of erosional surface dipping towards the WSW highlighted by a sharp grain-size break and mudstone clasts (see Part A for the location of this bed surface).

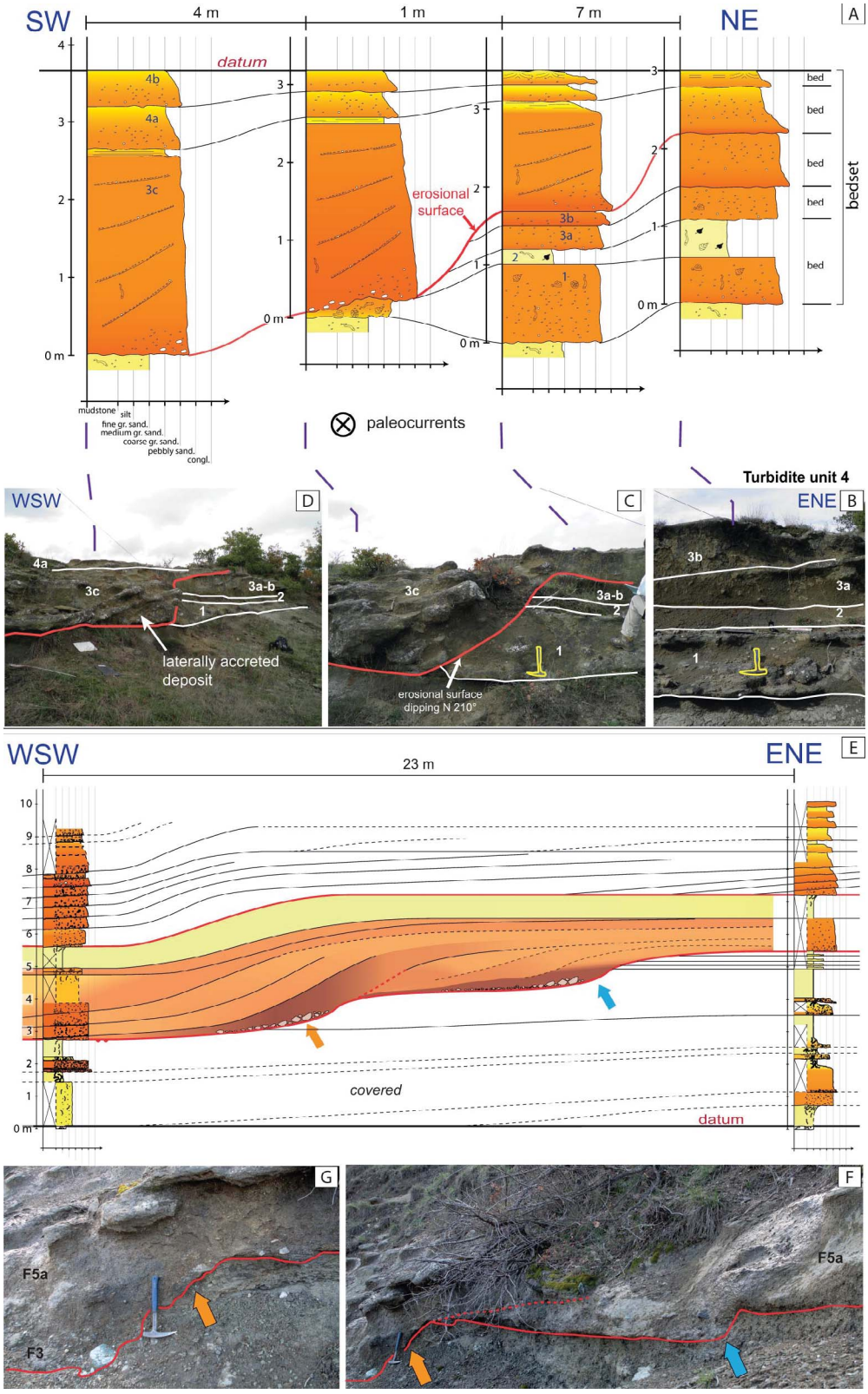

FIG. 8.—**A)** Detailed stratigraphic cross section of turbidite Unit 4, in which a well-developed erosional surface and associated beds dipping to the WSW can be observed. **B**–**D)** Details showing the lateral facies change. In particular, it is interesting to note that laterally accreted deposits dipping to the WSW are well developed against the high-angle erosional surface dipping in the same direction (see Parts C and D). **E)** Detailed stratigraphic cross section of turbidite Unit 1, in which a well-developed erosional surface and associated sigmoidal beds dipping to the WSW can be observed (see Figs. 3 and 10 for the location of this turbidite unit). **F**, **G)** Details of the basal erosional surfaces dipping to the WSW.

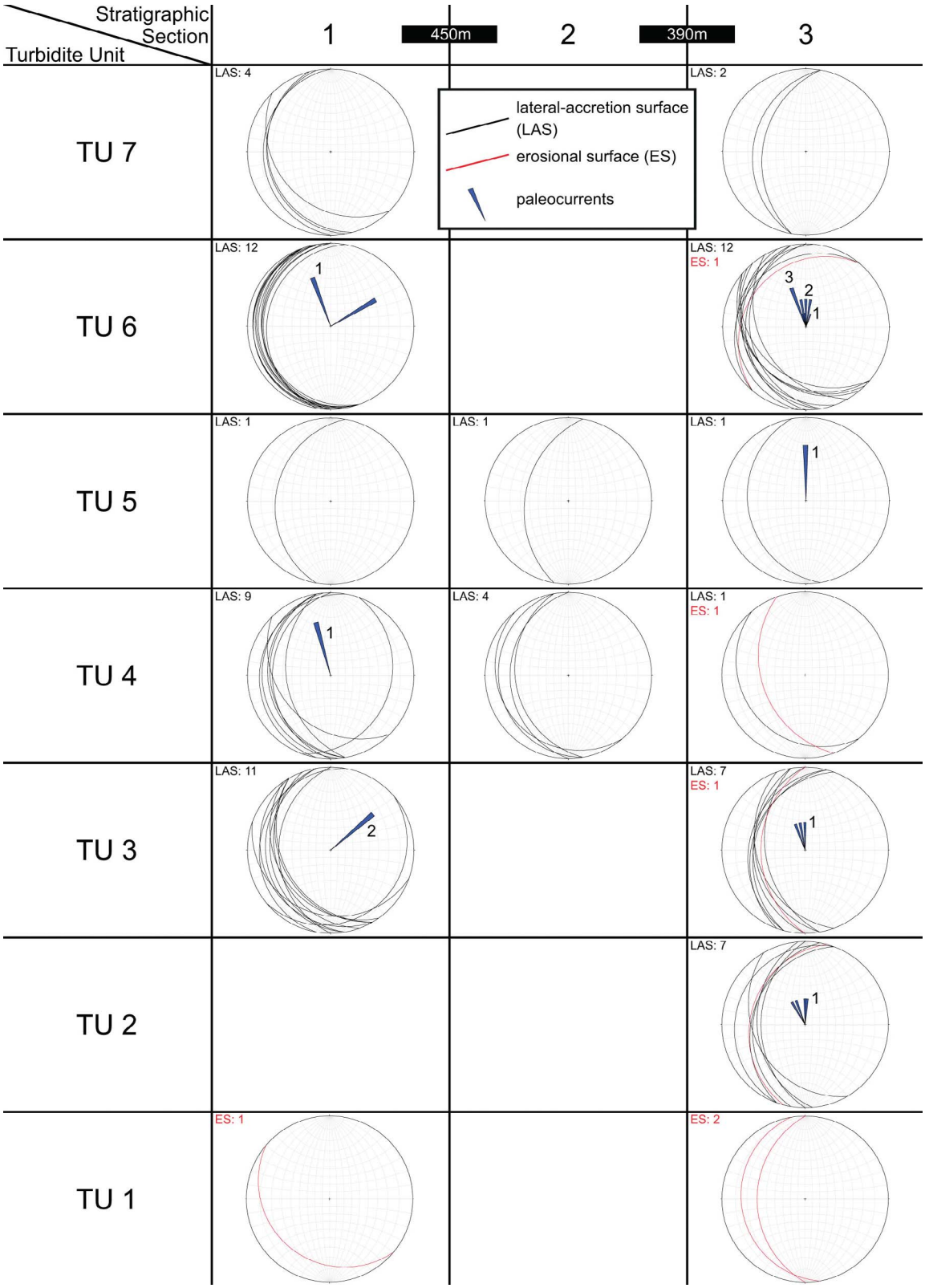

FIG. 9.—Diagrams illustrating the dip direction of turbidite beds (blue color) and erosional surfaces (red color) in all seven turbidite units (1 to 7) in logs 1, 2, and 3. Rose diagrams illustrating the paleocurrents derived from the flute casts at the base of the sandstone units are also given. Worth noting is that the dip directions of laterally accreted beds and erosional surfaces are all dipping to the WSW, perpendicular to the paleocurrents directed towards the N-NNW.

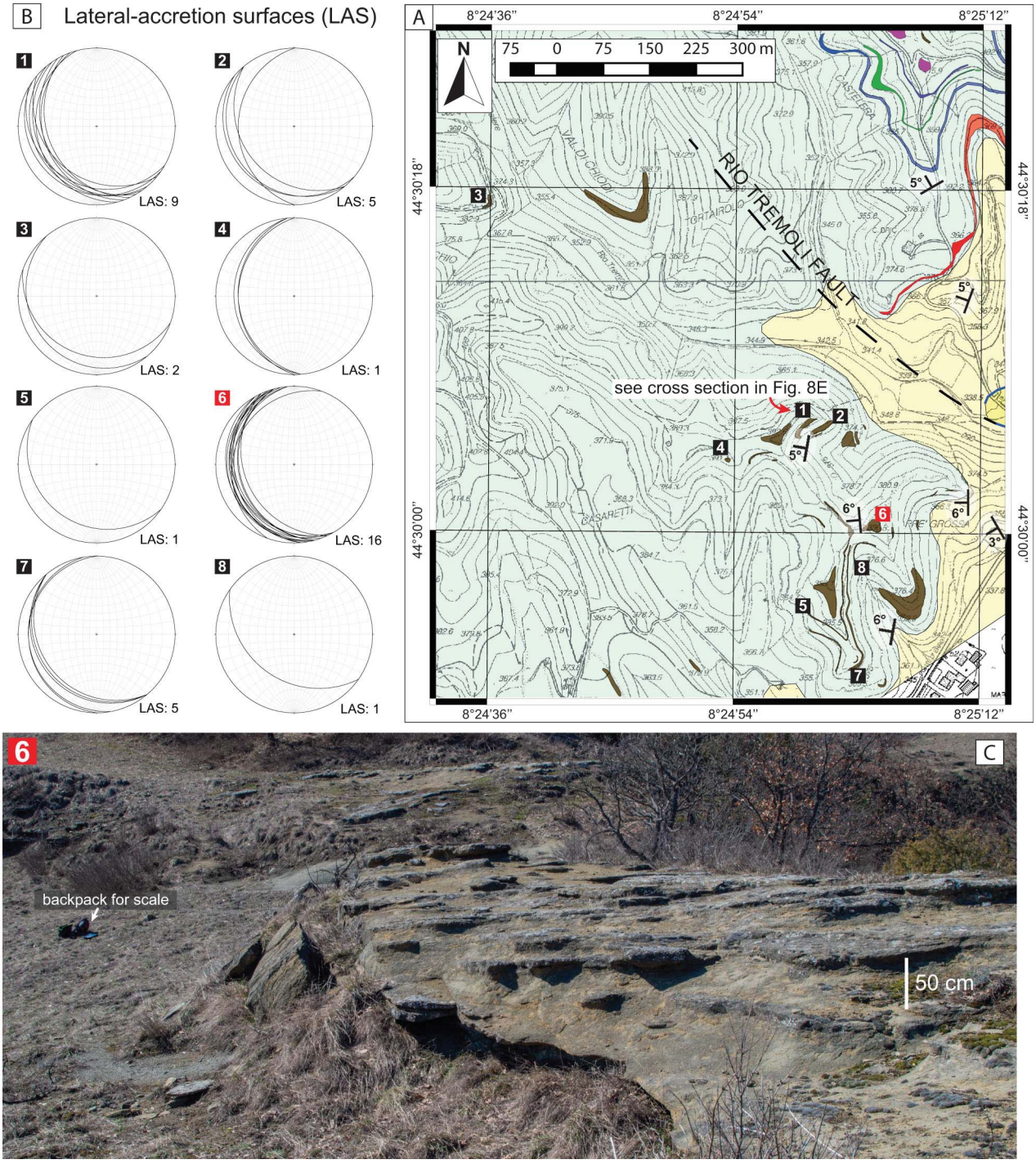

FIG. 10.—**A)** Geological map of the southern part of the study area where eight laterally accreted turbidite deposits controlled by the Rio Tremoli fault, parallel to the Garbarini fault, are shown (see Figs. 2A and 3 for the location map). **B)** Diagrams illustrating the dip direction of turbidite beds (blue color) and erosional surfaces (red color) of the laterally accreted turbidite units illustrated in Part A. **C)** Magnificent example of laterally accreted deposits all dipping towards WSW characterizing the sixth turbidite unit (see also Parts A and B).

perpendicular to the inclined bedding surfaces, all roughly dipping toward the WSW (see Figs. 9, 10). Furthermore, in a cut perpendicular to the paleocurrents, the erosional bases of the beds become more prominent to the ENE (i.e., towards the onlap surface associated with the Garbarini structural high) and always dipping to the WSW and NW (Figs. 5F, 6, 8). As regards this point, it is also important to remark that no erosional surfaces dipping in the opposite direction, i.e., to the ENE, have ever been detected. In the same way, all graded beds characterizing the large-scale sandstone units show an increase in grain size to the ENE, reaching the coarsest sizes towards the onlap surface near the Garbarini reverse fault and especially against the erosional bases of the beds (Figs. 6, 7, 8). This evidence can be observed well in Figure 6 showing that Unit 3 is composed

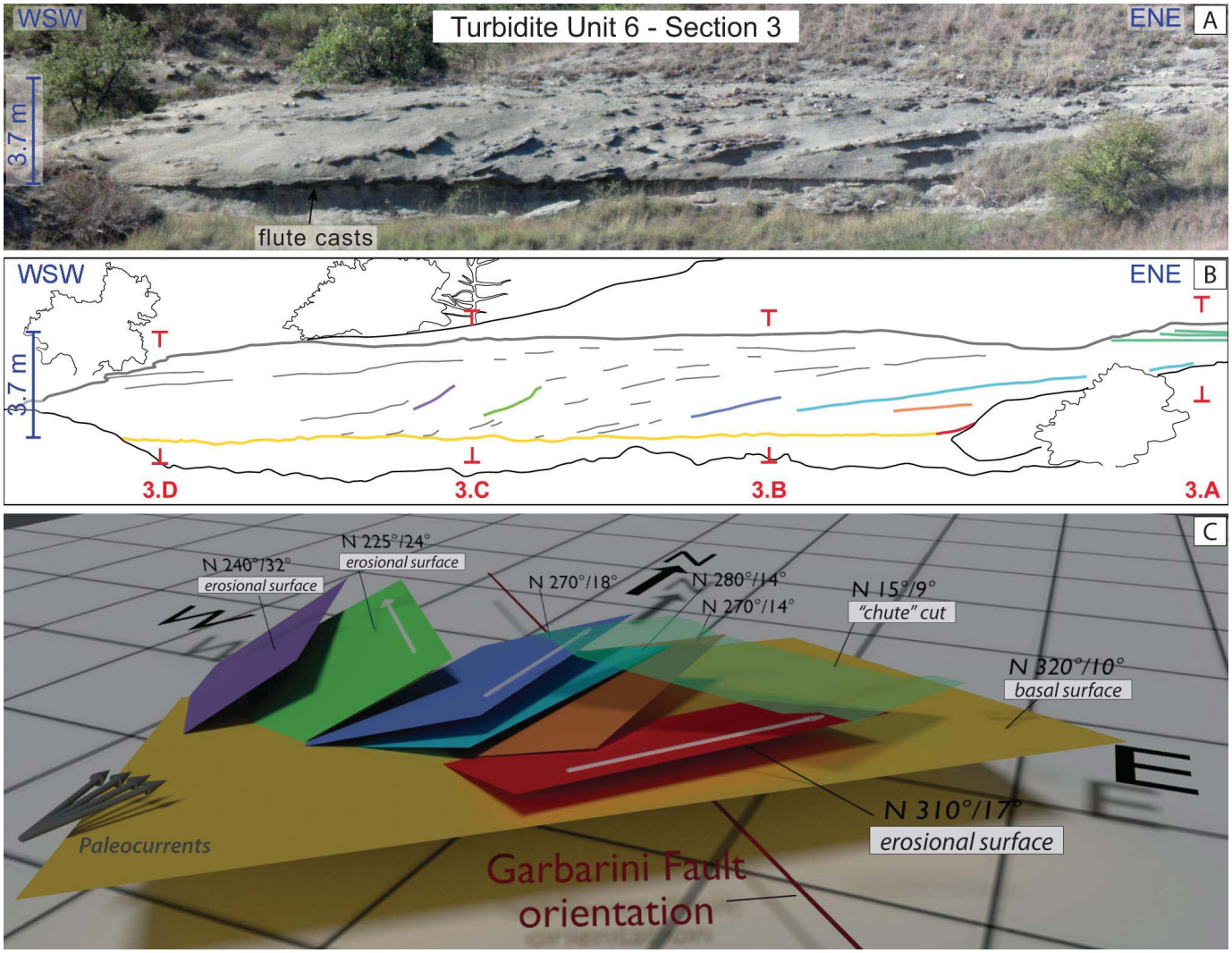

FIG. 11.—**A)** Panoramic view of sandstone Unit 6 (see also Fig. 7) showing well-developed laterally accreted beds dipping WSW (see Figs. 3 and 4 for the location of this Unit). **B)** Line drawing of Unit 6 shown in Part A, highlighting the main bed west-southwestward-dipping surfaces; the colors are the same as in the 3D surfaces shown in Part C. **C)** 3D view of the main bed dipping planes in which a rotation towards the NW of strike directions (roughly parallel to the paleocurrents) can be observed. The stratigraphic logs of Figure 7A are also shown in Part B.

of five graded beds, each one of which is characterized by a decrease in grain size towards the WSW, i.e., away from the paleo-topographic high.

Essentially, the detailed facies analysis of the large-scale sandstone units and of the graded beds composing them shows that the lateral-accretion surfaces can be related not only to erosional bases but also to lateral and vertical facies changes, within each lenticular turbidite bed; these changes are highlighted by WSW-ward-dipping sharp surfaces through which a decrease in grain size (towards the same dip direction) is also recorded.

Finally, it is important to remark that laterally accreted deposits, mainly formed by facies F3, F2, and F5, can pass laterally, towards the west and northwest, into low-angle to tabular beds usually characterized by facies F5b, F8, and poorly developed F9 (see Fig. 12C). Indeed, the equivalent deposits of units 4 and 5, about 0.7 km west from logs 3a and 3b, are tabular beds composed of F5 facies onlapping towards the east (see Fig. 4B, C). In some cases, these deposits, near the structural high, can be eroded by the successive coarse-grained graded beds (facies 1, 2, and 3) producing another set of laterally accreted deposits, as shown in Figure 13A and B.

Laterally Accreted Sandstone Units Related to Dense Flow Deflections

The evidence that these turbidite sandstone units are characterized by well-developed lateral accretions perpendicular to the paleocurrents has led to interpret these deposits as point bars associated with meander belts (see Mutti and Normark 1991; Mutti et al. 2002; Janocko 2011).

However, laterally accreted deposits—well developed only in a limited zone (few hundred meters wide) to the south of the Garbarini structural high—the strata and erosional surfaces all dipping towards the WSW and the asymmetrical cross-current facies tract (perpendicular to the NW-oriented Garbarini structural high), suggest a close relationship between these deposits and the location and orientation of this structural high, casting doubts on the occurrence of a meander belt. Consequently, all this evidence, together with the fact that the paleocurrents are directed towards the N, i.e., perpendicularly to the bedding dip and roughly oblique (at low angle) to the Garbarini structural alignment, prompts an alternative interpretation, according to which the turbidite units of the Fraschetto turbidite system could be formed by lateral juxtaposition of sharp-based,

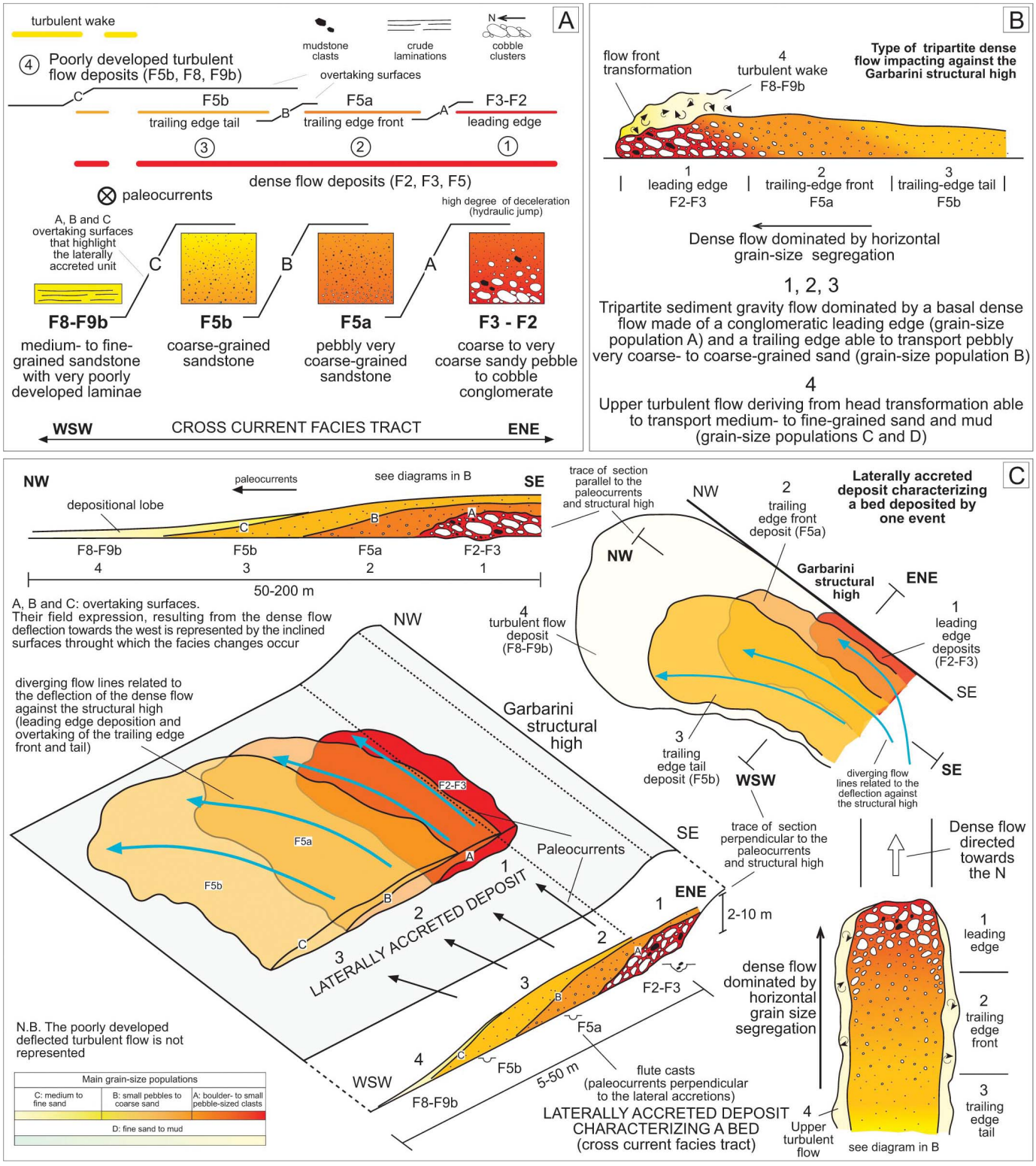

FIG. 12.—**A)** Cross-current facies tract characterizing the west-southwestward-dipping beds forming the laterally accreted deposits. **B)** Type of composite sediment gravity flow characterizing the deposition of Fraschetto turbidite units. **C)** General model that explains the formation of the cross-current facies tract shown in Part A and associated laterally accreted deposits, in relation to the deceleration and deflection of a longitudinally segregated dense flow against the Garbarini structural high.

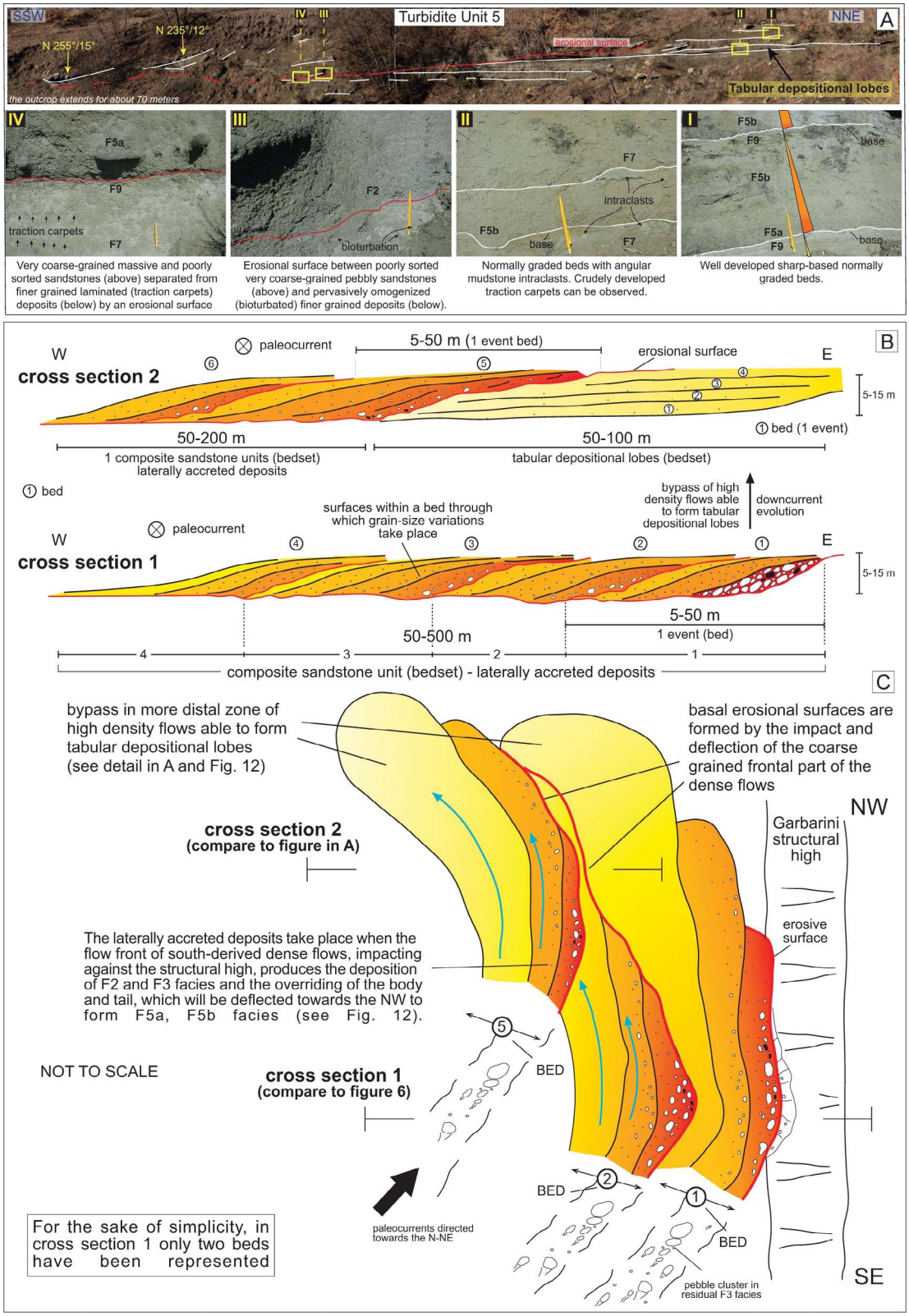

FIG. 13.—**A)** Detail of the turbidite sandstone Unit 5 in the area of log 3, where it can be observed that tabular turbidite beds are truncated by a relatively high-angle erosional surface associated with coarse-grained, laterally accreted deposits dipping toward the SSW. See Figure 3 for the location of the logs and outcrops. **B)** The diagram below shows an example of a large-scale laterally accreted sandstone unit composed of five beds dipping WSW (compare to Figs. 5, 6); conversely, the diagram above shows tabular depositional lobes eroded by coarse-grained graded beds that form well-developed laterally accreted deposits (compare to Part A). The depositional lobes characterized by facies 4 can be deposited by the upper turbulent flows that bypass the proximal coarse-grained laterally accreted deposits. **C)** Diagram showing the formation of the laterally accreted deposits and related sandstone tabular lobes in relation to deflections processes induced by a NW–SE-oriented structural high (compare to Fig. 12). The traces that can represent the cross sections indicated in Part B are also shown.

normally graded beds deposited by sediment gravity flows deflected by the Garbarini structural high, as illustrated in Figures 12 and 13.

The coarse-grained massive facies can indeed be interpreted as related to the downcurrent evolution of a dense flow (in the meaning of Mutti et al. 1999, 2003 and Tinterri et al. 2003, 2020), i.e., a sediment gravity flow characterized by a high sediment concentration that tends to suppress the turbulence and where the main mechanisms of particle support are essentially related to an interplay of grain-size concentration, overpressure, and matrix strength (see Middleton and Hampton 1973; Lowe 1979). These types of gravity flows, which can derive from resedimentation processes characterizing the southern tectonically-controlled basin margin (i.e., the Mioglia fault; see Fig. 2), are interpreted as surge-type high-energy dense flows that, generally, are not prone to produce a meandering process dominated by helical flows (e.g., Mutti et al. 2003, 2009; Kolla et al. 2007). In particular, these flow types, which can be similar to the flowing grain layers by Sanders (1965) or sandy debris flows by Shanmugam (1996), are generally dominated by longitudinal grain-size segregation (i.e. the horizontal grain segregation prevails over the vertical one), with the coarsest grain sizes that tend to be concentrated in the leading edge of the flow, where intergranular friction dominates, while the finest ones are concentrated in the trailing edge of the flow (i.e., body and tail), where pore-fluid pressure tends to dominate (see Mutti et al. 1999; Major and Iverson 1999; Sohn et al. 1999, 2002; see also Fig. 12B). Therefore, these gravelly dense flows can be interpreted as tripartite composite gravity flows characterized by 1) a body in which pore-fluid pressure is developed and maintained during mobilization and motion of the flow, 2) a head in which grain-contact friction and bed friction cause the deposition of the frontal part of the flow (F3 deposits, Fig. 12), and 3) an upper turbulent flow derived from the head transformation due to the shear stress exerted by the displacement of the ambient fluid (see Marr et al. 2001).

The lateral facies tract in Figure 12A takes place when the flow front of south-derived tripartite flows (Fig. 12B), impacting against the NW-oriented Garbarini structural high characterized by a steep gradient, produces the deposition of the orthoconglomerate (F3) and the overriding of the body and tail, which will then be deflected to the NW by the structural high. The bypass and related deflections of the trailing edge of the flow characterized by longitudinal grain-size segregation can have produced lateral juxtaposition of two different types of F5, which, from ENE to WSW, are a coarser F5a, composed of pebbly very coarse sands, and a finer F5b, composed of coarse-grained sands (Fig. 12A, C). Consequently, the well-developed WSW-dipping surfaces, which can be observed in a cross-current cut, must be related not only to the erosional bases, but also to the overriding-bypass surfaces that are recorded by the internal bed surfaces along which facies changes occur (see surfaces A, B, and C in Fig. 12A, C). The deflection of these different parts of flow, due to the NW-oriented Garbarini high, is also supported by the progressive rotation of bed strike directions to the NW (see Fig. 11). Indeed, bed strike orientations can be considered roughly parallel to the paleocurrents and the progressive change from NE to NW of erosional bases and bed surfaces (see Fig. 11C) can be related to the progressive northwestward deflection of overriding trailing-edge surges (see Fig. 12C). In particular, these overriding processes can also explain the N–S-oriented erosion in Unit 6, filled with tabular beds, which can be interpreted as a sort of cutoff (see Figs. 7A, C, 12C).

At the same time, the high shear stress exerted by the ambient fluid and the fluidization processes related to water injections at the base of the flow front can partially transform the leading edge of the dense flow, generating turbulence and an affiliated turbulent wake (*sensu* Mohrig and Marr 2003 and Marr et al. 2001), which, in turn, will be deviated in directions ranging between W and NW. Despite having a relatively limited role compared with that of dense flows, this process can form tabular beds that can be interpreted as depositional lobes mainly composed of facies F5b, F8, and F9 (Fig. 12). The lateral westward deposits of units 4 and 5 are tabular lobes always onlapping towards the east (see Figs. 4B, C), whereas, near the structural high, these tabular beds can be eroded by the successive dense flows that produce the high-angle erosional surfaces (all dipping towards the WSW, Fig. 13) always associated with well-developed laterally accreted deposits formed by the lateral juxtaposition of graded beds (see Fig. 8, 13). Moreover, the process of head transformation can also be considered important for the formation of the flute casts found at the bases of sandstone units, which indicate paleocurrents towards the N and NNW and, thus, allow these WSW-dipping surfaces to be interpreted as laterally accreted deposits.

In conclusion, this simple depositional model, essentially based on the way in which a bipartite dense (debris-flow-type) flow can form a sharp base normally graded bed (e.g., Mutti et al. 1999, 2009), can account for the sedimentary characteristics described in the previous section. Furthermore, the fact that these lateral accretions are particularly evident only near the southern limb of the Garbarini structural high further supports that they are strictly related to the dynamics of bipartite dense flows, in accordance with the size and orientation of the structural high that, favoring a low angle of incidence of the flow, can promote lateral deflection and associated laterally accreted deposits (see Figs. 12C, 13).

THE STRUCTURALLY CONTROLLED MIOGLIA MINI-BASIN: A DEPOSITIONAL MODEL

The stratigraphic framework of Figures 2 and 4 shows that the Fraschetto sandstone units were deposited in a structurally controlled depocenter, mainly controlled by the NE Garbarini fault (see Figs. 2A, C) and very likely by other parallel faults, as indicated in Figures 3 and 10. The stratigraphic cross section in Figure 4 shows evident stratigraphic pinch-outs, angular unconformities, and onlap towards the ENE, i.e., against the Garbarini structural alignment. This evidence, together with the essential disappearance of these turbidite units to the north of the Garbarini fault (see Fig. 3), shows that this structural high must have acted as a morphologic threshold for the south-derived longitudinally segregated dense flows and that the laterally accreted deposits must have been controlled by these NNW–SSE-oriented faults. In particular, as it was produced by a normal fault successively inverted (Fig. 2C), this structural high must also be characterized by a high angle and steep morphology, and tectonic inversion must have started during the deposition of the uppermost part of M1 or, at the most, of the basal part of the M2 unit, as testified by the growth wedge that can be observed along the Mioglia flexure (see Fig. 2A).

This supports the interpretation that the dense bipartite flows forming the Fraschetto turbidite sandstones could derive from the gravity remobilization of the Molare 1 deposits along the fault-controlled southern basin margin, which may be represented by the Mioglia fault (see Fig. 2C, D). From this point of view, the very small coarse-grained sandstone units of the Fraschetto turbidite system are mainly controlled by the Mioglia and Garbarini faults, which respectively triggered and steered the evolution of the sediment gravity flows (Fig. 2A, C). More precisely, since the Fraschetto units indicate paleocurrents coming from the south, resedimentation processes affecting the southern fault-controlled basin margin, which is represented by the Mioglia structural alignment, could produce sediment gravity flows able to evolve towards the north against the Garbarini structural high, complicated by other minor parallel faults (see Figs. 3, 10, 14), producing laterally accreted deposits according to the model shown in Figures 12C, 13B, and 14. Furthermore, the structural depressions created by these normal faults successively inverted could favor the funnelling and the deflection of the sediment gravity flows towards the NNW, facilitating the formation of laterally accreted side bars characterized by an asymmetrical cross-current facies tract as illustrated in the depositional model of Figure 14.

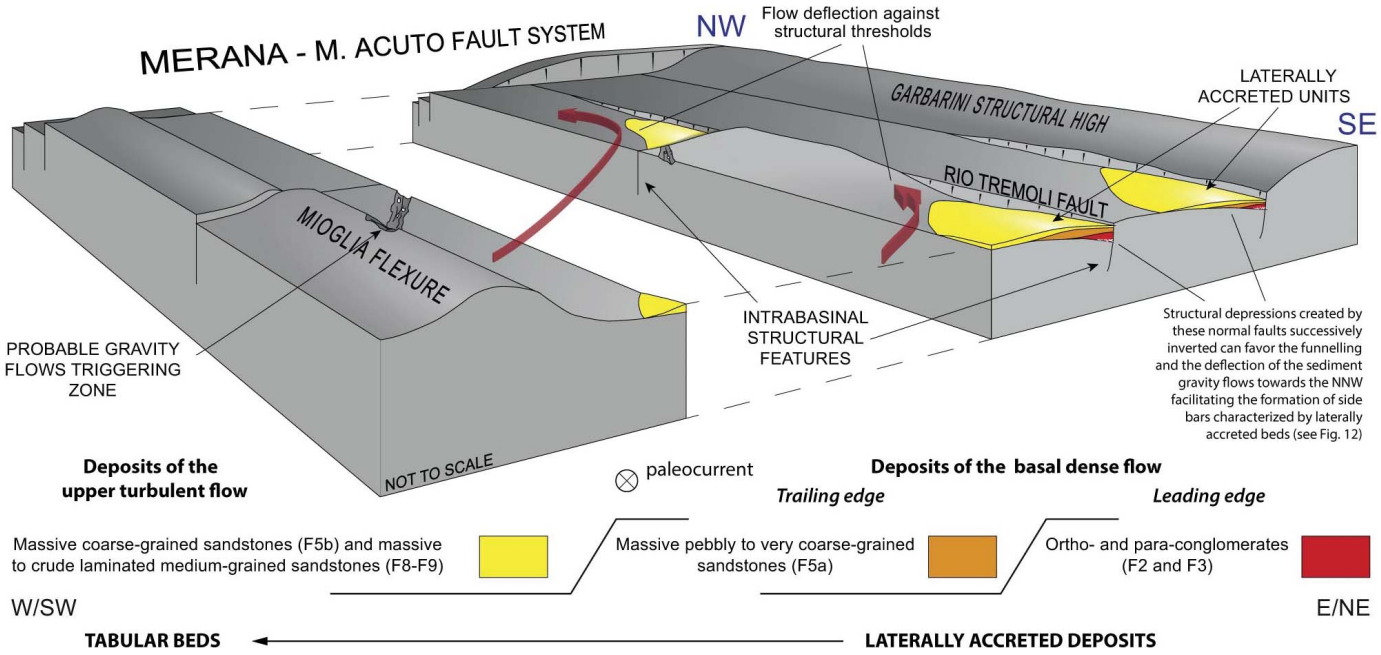

FIG. 14.—Paleogeographic model of the Mioglia basin at the time of the deposition of the laterally accreted Fraschetto turbidite units.

Essentially, the Fraschetto turbidite system can be interpreted as a Type A mixed system (*sensu* Mutti et al. 2003), i.e., a small sand-rich depositional system characterized by short-lived, coarse-grained and extremely poorly organized deposits derived from sediment failures and trapped in adjacent small fault-bounded depressions. These systems can thus be seen as immature, marginal, and poorly efficient turbidite-like systems (*sensu* Mutti et al. 1999) forming seaward of, but adjacent to, feeder delta complexes and, consequently, forming at shallower depth than that of classic basinal turbidites. The Fraschetto turbidite units (i.e., M2 group, Fig. 2) are indeed encased in siltstones rich in shallow-water trace fossils and macroforaminifera, which can be interpreted as distal prodelta deposits in a shelf environment (see Fig. 2). The latter deposits can be related to the time-equivalent deltaic systems reported by Rossi et al. (2009) in an area located to the southwest of the uplifting Mioglia structure (Fig. 14). From this point of view, the very coarse grain-size populations characterizing the Fraschetto turbidite units (see Fig. 12) can be further evidence that they must derive from remobilization of the underlying M1 fan-delta deposits, rather than directly from hyperpycnal flows triggered by floods entering seawater, since these processes generally produce delta-front sandstone lobes made of fine-grained sandstones (Mutti et al. 1995, 1996), whose northeastward evolution could also be hindered by the growth of the Mioglia structure.

In conclusion, the geological setting, the small size, and the tectonic confinement of the basin in an outer-shelf environment, together with the low efficiency of sediment gravity flows, particularly favored entrapment of coarse-grained sand, allowing the Mioglia basin, at the time of M2 deposition, to be interpreted as a tectonically controlled intra-shelf mini-basin (see Fig. 14).

DISCUSSION

Control of Basin Morphology on Flow Evolution and Flow Efficiency: a Comparison to other Confined Turbidite Systems

This work shows that deflection processes of bipartite dense flows with very low efficiency in highly confined basins can produce laterally accreted deposits. The influence of tectonically controlled morphologies similar to that of this work on turbidite sedimentation has been discussed through field studies (e.g., Remacha et al. 1998, 2005; Mutti et al. 1999; Haughton 2000; Amy et al. 2004; Hodgson and Haughton 2004; Mutti and Tinterri 2004; Kane et al. 2010; Bell et al. 2018; Cullen et al. 2019), subsurface seismic studies (e.g., Normark 1985; Maier et al. 2018; Howlett et al. 2021), and experimental studies (e.g., Soutter et al. 2021). Recently, however, asymmetrical cross-current facies tracts associated with the geometry of the basin have been discussed in detail by Tinterri et al. (2017) in various turbidite systems characterized by different efficiencies (see also Tinterri and Tagliaferri 2015; Cunha et al. 2017; Tagliaferri et al. 2018; Tinterri and Piazza 2019).

In general, the flow efficiency can be seen as the ability of the flow to carry its sediment load basinward and to segregate its grain-size populations into well-developed and distinct facies over distance (Mutti et al. 1999). All things being equal, this depends on the ability of the basal dense flow to transform itself, i.e., to form a horizontal grain-size segregation and to allow a leading-edge transformation producing an upper turbulent flow that can transport finer grain-size populations farther downcurrent. Besides the original character of the parent flow, the geometry and the degree of basin confinement can alter flow efficiency, through deceleration and suppression of flow evolution (Tinterri et al. 2016, 2017). From this point of view, three main degrees of efficiency can be distinguished (see Mutti et al. 2003): 1) highly efficient flows characterized by bipartite flows dominated by an upper turbulent flow; these flows generally tend to characterize large foredeep basins, such as those in the northern Apennines (Italy). 2) Intermediately efficient flows, in which bipartite flows are dominated by a basal dense flow; in these cases, the basin confinement favors decelerations and flow decoupling of upper turbulent flows (see Tinterri and Tagliaferri 2015). These flows tend to characterize confined wedge top basins or inner foredeeps and correspond to Type B turbidite mixed systems by Mutti et al. (2003). 3) Low-efficiency flows, in which the dense flow is not able to produce an efficient upper turbulent flow and the deposits are dominated by massive coarse-grained sandstones related to longitudinally segregated dense flows. These are deposited in very small tectonically confined basins and can correspond to Type A turbidite mixed systems by Mutti et al. (2003).

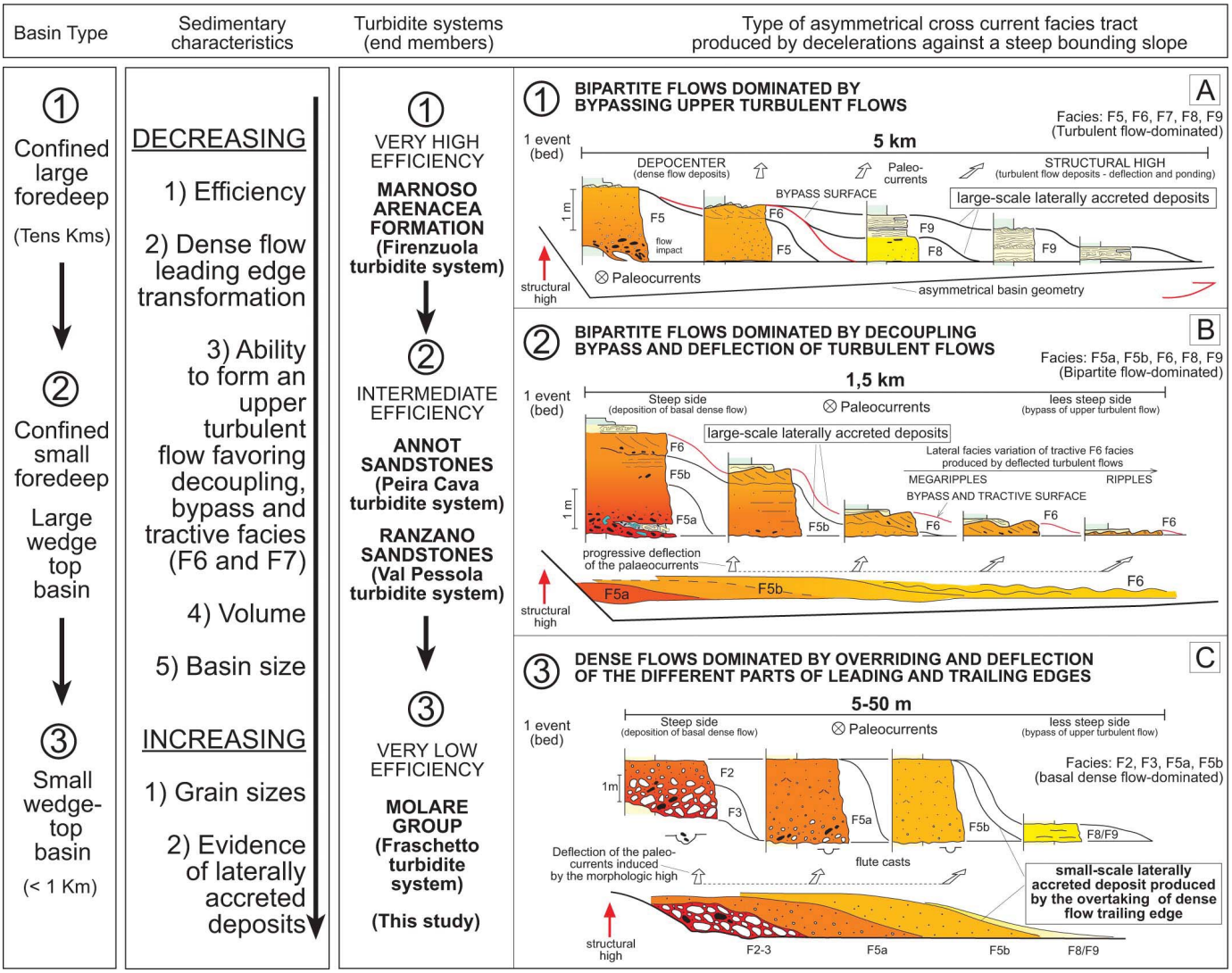

FIG. 15.—Types of cross-current facies tracts and laterally accreted deposits related to efficiency degree (*sensu* Mutti et al. 1999), tectonic confinement, and basin sizes. Worth noting are the similarities to the facies tract and processes discussed in this study. The main references are: **A)** Firenzuola turbidite system in the Marnoso–Arenacea Formation (northern Apennines, Italy) (Tinterri and Muzzi Magalhaes 2011; Tinterri and Tagliaferri 2015; Tagliaferri and Tinterri 2016); **B)** Annot Sandstones in the Peïra Cava basin (southwestern France) (Tinterri et al. 2016; Cunha et al. 2017) and Ranzano Sandstones (northern Apennines, Italy) (Tinterri et al. 2017); **C)** this work. The colors represent the grain-size populations (see Fig. 12).

However, sediment gravity flows with different efficiency degrees can experience similar cross-current processes due to the decelerations produced by bounding slopes parallel or at a low angle with respect to flow direction, resulting in various types of asymmetrical cross-current facies tracts characterized by different scales (i.e., lateral extent) depending on their efficiency (see Fig. 15A, B). These cross-current facies tracts are similar to the one presented in this work (Figs. 12A, 15C), which can be considered the low-efficiency end-member case where the deposits are dominated by a longitudinally segregated dense flow that is not able to produce a large-volume upper turbulent flow. In this case, the impact of dense flows against a structural high is able to produce well-developed lateral accretions of graded beds, due to the deposition of the coarse-grained flow front to form F3 and F2 facies, and to the overtaking and lateral deflection of the body and tail of the flow, which deposit various types of laterally juxtaposed massive F5 having different grain-size distributions (F5a and F5b in Fig. 12, see also Tinterri et al. 2017).

Furthermore, similar local tectonic controls on basin geometry and flow processes have also been documented through detailed subsurface studies in the Angola offshore (Oluboyo et al. 2014; Howlett et al. 2021) and in the California offshore, such as in the Monterey Fan (Normark 1985) and in the Catalina Basin (Maier et al. 2018). The work by Maier et al., in particular, can fit very well with the sedimentation models described by Tinterri et al. (2016, 2017) and, although at a different scale, even with the model presented in this work (see Fig. 14). Indeed, Maier et al. (2018) highlighted that seafloor morphology, distribution of depositional and erosional features, and location of depocenters in the channel–lobe transition of the Catalina Basin are strongly controlled by shifting confinement and seafloor gradient related to inherited basement structures, active faults, and basin margins. In this study, flows entering the basin from the northeast through the San Gabriel channel are turned to the northwest by northwest–southeast-oriented structural relief along the southern basin margin. Steep relief at the basin margins, persistent down-basin gradients, and increasing confinement from the narrowing basin are factors that

control flow directions and funnel fan sediments to the northwest in elongate lobe packages that onlap and are contained by basement highs. Here, ponded stacked lobes are characterized by a map-view distribution and thickness trends determined by the basin shape.

More recently, laboratory experiments by Soutter et al. (2021) on the influence of orientation of confining topography on turbidity currents have reproduced deposits that can be compared to those of this study. More precisely, a morphology oblique to the incoming flow caused the deflection and acceleration of the high-density basal part of the flow along the barrier. Concurrently, the forced deceleration at the barrier, with the possibility of producing a granular jump (*sensu* Smith et al. 2020), resulted in thickened deposition on the slope characterized by high-angle inclined strata (Soutter et al. 2021, see their Figures 10 and 12).

Consequently, all these similarities are important grounds that can reinforce the interpretation of lateral-accretion processes related to a bounding slope, rather than to a meandering channel.

Evidence in Favor of the Lack of a Meandering Channel and Supporting Flow-Deflection Model

In addition to the discussion in the previous section, the interpretation of laterally accreted deposits related to a bounding slope is supported by other evidence, such as lateral accretions and erosional surfaces dipping only towards the WSW as demonstrated by the data from all the sandstone units in the studied basin, which today is about 2 km^2, or the fact that the coarse-grained facies and erosional surfaces are all concentrated towards the ENE, i.e., towards the Garbarini morphological high (Figs. 5, 6, 8), and the fact that these types of deposits disappear out of this very small tectonically controlled basin (Figs. 2, 3).

As regards the first item of evidence, if the lateral-accretion deposits were related to a meander belt, beds and erosional surfaces dipping in opposite directions should be found, recording the different bends of a meandering channel. Even though work on fluvial environments has shown that asymmetrical tectonic tilting can produce a migration of the channels towards the fault, favoring the formation of asymmetrical meandering belts with preferential dip of lateral-accretion units (e.g., Leeder and Alexander 1987; Peakall et al. 2000), it should be taken into account that, in this case study, 100% of the lateral-accretion deposits and erosional surfaces dip to the WSW, i.e., away from the structural high (Fig. 9), and cases in which the totality of the lateral-accretion surfaces dip in only one direction are very unlikely (Peakall et al. 2000). Furthermore, it should also be taken into account that the involved scales and processes are completely different (e.g., Kane et al. 2010; Hubbard et al. 2014, 2020); in other words, the dynamics of a diluted turbulent flow in a long-lived, large scale (tens of kilometers long) meandering belt in fluvial and deep marine environments (e.g., Schumm et al. 2000; Peakall et al. 2000; Abreu et al. 2003; Pirmez and Imran 2003; Wynn et al. 2007) is not comparable with the dynamics of a surge-type or short-lived high-energy gravelly dense sediment gravity flows in a very small intra-slope basin (a few kilometers wide) as in the case of this work (e.g., see type A mixed system by Mutti et al. 2003). In particular, as regards this work, it is not clear how a meander channel characterized by a western outer side, as it should be in this case (see, for example, Fig. 7), could always produce erosional surfaces and massive coarse-grained and conglomeratic facies related to non-turbulent dense flows towards the east, i.e., exactly on the opposite inner side (e.g., Figs. 5, 6, 8, 9). On this point, it should also be taken into account that a helical flow in a dense flow, rheologically similar to a sandy debris flow, is not credible at all, also because a flow of this type decelerating against a steep bounding slope (irrespective of whether it is a channel side or a topographic high) should simply impact, deposit and, at the most, move along the tectonically controlled steeper part of the basin as shown in many field works (e.g., Remacha et al. 1998; Mutti et al. 1999; Amy et al. 2004; Tinterri et al. 2017; Cunha et al. 2017), seismic studies (e.g., Maier et al. 2018), and laboratory experiments (Soutter et al. 2021). After all, the literature reports an extensive and often controversial debate on the dynamics of meandering flows in deep marine channel bends (e.g., Corney et al. 2006; Imran et al. 2007; Sumner et al. 2014; Azpiroz-Zabala et al. 2017), which often leads to controversial interpretations of the nature and origin of lateral-accretion deposits (e.g., Pickering et al. 2001; Maier et al. 2012, 2013; Fildani et al. 2013; Tinterri and Civa 2014; Bayliss and Pickering 2015; Pickering and Hiscott 2016). These authors, in particular, have shown that the presence of inclined reflections or beds in a deposit is necessary but insufficient grounds to demonstrate lateral accretion and that not always do these features imply the occurrence of a meander or high-sinuosity turbidite channels. Maier et al. (2012, 2013) argue that the point-bar interpretation should not be used if clear differences, in term of scales, geometries, and facies types and distributions exist between the studied deposits and those reported in fluvial and deep-water meandering channels (see above).

From this point of view, the interpretation presented in this work (see Figs. 12, 13) can account for the sedimentary characteristics of the studied laterally accreted deposits and, if we really want to make a comparison to fluvial or channelized strata, these deposits could be similar to a sort of side bar rather than a point bar, where the low-angle incidence of a series of dense bipartite flows can produce lateral juxtaposition of graded beds that form the laterally accreted deposits (see Figs. 12, 13). Indeed, these types of deposits are always associated with the Garbarini fault system, where a series of structural depressions can favor the funnelling and deflection of the sediment gravity flows (see Fig. 14). A fairly similar interpretation has been advanced by Bayliss and Pickering (2015) (see also Pickering and Hiscott 2016) for the coarse-grained lateral-accretion deposits of the Morillo turbidite system (south-central Pyrenees). These authors argue that it is very unlikely that these deposits can be the expression of a point bar related to a high-sinuosity channel system because they are generated by gravelly-dense flows in a small highly confined basin characterized by relatively steep seafloor gradients due to the submarine growth of various anticlines. Rather, the authors advance the hypothesis that these types of deposits are interpreted as a sort of attached side barform; indeed, in these settings, it is more than plausible to think that the deflection of these high-energy and catastrophic dense flows can occur, especially if the depositional system is constrained by steep morphologies, which are generally controlled by tectonics.

Therefore, all the evidence shown in this work tends to support a depositional model in which well-developed laterally accreted deposits are associated with low-efficiency, sand-rich sediment gravity flows, the deposition from which is steered by structurally controlled steep slopes characterizing small confined basins. In these settings, these types of flows can produce the lateral juxtaposition of graded beds, each one of which is characterized by a well-defined cross-current facies tract that can be considered the typical expression of bipartite flows decelerating, with a low angle of incidence, against a steep bounding slope (Figs. 12, 13). The fact that these laterally accreted deposits are fully evident especially in this structurally controlled small turbidite system, and not in those having larger volumes and higher efficiency, must depend on the basin scale and on a relationship between a low efficiency degree and a particular arrangement of fault-controlled morphological highs; i.e., in these small systems, the relation between type of flow, size, and orientation of the bounding slopes with respect to the flow direction of incidence must be particularly favorable in order to constrain the flow evolution highlighting the overriding surfaces and the bed-scale lenticular geometries produced by flow deflections (see Figs. 12, 13, 15).

CONCLUSIONS

This work discusses well-preserved laterally accreted deposits characterizing low-efficiency sand-rich turbidites in a small tectonically

controlled basin located in the western part of the wedge-top Tertiary Piedmont Basin in NW Italy (see Figs. 1, 2). These lenticular coarse-grained and poorly sorted sandstones (2–6 m thick and 50–500 m wide) are characterized by well-developed laterally accreted deposits formed by the lateral juxtaposition of graded beds (0.5–2 m thick and 5–50 m wide), all dipping towards WSW, and with the lateral facies tract shown in Figure 12. These deposits, characterized by paleocurrents towards the N, are mainly controlled by the NW–SE-oriented structural highs (see Figs. 3, 5, 14) that induced lateral deflection of very-low-efficiency dense flows generated by resedimentation processes affecting the underlying fan-delta deposits along the southern fault-controlled basin margin (Fig. 14). The rapid deceleration of these south-derived and longitudinally segregated bipartite flows against the tectonically controlled bounding slope to the north (Figs. 3, 14) produced the laterally accreted graded beds through the deposition of the coarse-grained flow front to form F3 and F2 facies, and the consequent overriding and lateral deflection towards the west of the body and tail of the flow, which deposited laterally juxtaposed F5 with different grain sizes (F5a and F5b) and poorly developed F5b-F8-F9 facies that represent depositional lobes. The lateral juxtaposition of these graded beds forms the laterally accreted deposits presented in this study (see Figs. 12, 13).

Thus, this work shows that deflection processes in small-scale, highly confined structural depressions (< 1 km wide) can produce laterally accreted deposits. Furthermore, the comparison to other tectonically controlled turbidite systems characterized by higher degrees of efficiency suggests the possibility of a continuum of different types of cross-current facies tracts in accordance with their degree of efficiency (Fig. 15). Indeed, these facies tracts are all very similar in terms of lateral evolution and physical processes, thus showing that the case illustrated in this work can be an end member representing low-efficiency turbidite systems deposited in very small basins characterized by tectonically controlled steep bounding slopes. As a consequence, in these types of system, these features must be strictly related to the dynamics of dense bipartite flows in accordance with the size, geometry and orientation of the structural high, which, promoting low angles of incidence of the flows, can favor deflection processes and formation of laterally accreted deposits (see Fig. 15).

ACKNOWLEDGMENTS

We thank Emiliano Mutti for his teachings and constructive discussions throughout the years on turbidites and Tertiary Piedmont Basin. We are also deeply grateful to Davide di Biase for reading an earlier version of the manuscript and for the discussions about the onlap relationship of the basal part of Fraschetto turbidite system. We also wish to thank Gary Hampson (Editor), Andrea Fildani (Associate Editor), Katherine Maier, Fabiano Gamberi, and an anonymous reviewer for their very helpful and constructive comments, which helped to improve the manuscript. We are very grateful also to John Southard for his careful editing and comments on the final version of the manuscript. The comments by Massimo Rossi (ENI), Ian Kane, and Michal Janocko were also appreciated. We are also grateful to Fabrizio Diaz Lima, Alberto Piazza, Michele Laporta, and Fabrizio Storti for discussions in the field. This research was funded by ENI SpA and Petrobras (Petróleo Brasileiro S.A.). In particular, we thank Giancarlo Davoli and Denis Palermo (Eni) and Mário Carminatti and Pierre Muzzi Magalhaes (Petrobras).

REFERENCES

Abreu, V., Sullivan, M., Pirmez, C., and Mohrig, D., 2003, Lateral accretion packages (LAPs): an important reservoir element in deep water sinuous channels: Marine and Petroleum Geology, v. 20, p. 631–648.

Amy, L.A., McCaffrey, W.D., and Kneller, B.C., 2004, The influence of a lateral basin-slope on the depositional patterns of natural and experimental turbidity currents, *in* Joseph, P., and Lomas, S.A., eds., Deep-Water Sedimentation in the Alpine Foreland Basin of the SE France: New Perspectives on the Gres D'Annot and Related Systems: Geological Society of London, Special Publication 221, p. 311–330.

Azpiroz-Zabala, M., Cartigny, M.J.B., Sumner, E.J., Clare, M.A., Talling, P.J., Parsons, D.R., and Cooper, C., 2017, A general model for the helical structure of geophysical flows in channel bends: Geophysical Research Letters, v. 44, p. 11932–11941.

Bayliss N.J., and Pickering K.T., 2015, Deep-marine structurally confined channelised sandy fans: Middle Eocene Morillo System, Ainsa Basin, Spanish Pyrenees: Earth-Science Reviews, v. 144, p. 82–106.

Bell, D., Stevenson, C.J., Kane I.A., Hodgson D.M., and Poyatos-More, M., 2018, Topographic controls on the development of contemporaneous but contrasting basin-floor depositional architectures: Journal of Sedimentary Research, v. 88, p. 1166–1189.

Bernini, M., and Zecca, M., 1990, Le deformazioni nelle Formazioni di Molare e di Rocchetta (Oligocene–Miocene inferiore) della regione di Mioglia (SV) (Margine Sud del Bacino Terziario Piemontese): Atti Ticinesi di Scienze della Terra, v. 33, p. 1–10.

Campbell, C.V., 1967, Lamina, laminaset, bed and bedset: Sedimentology, v. 8, p. 7–26.

Cazzola, C., Fonnesu, F., Mutti, E., Rampone, G., Sonnino, M., and Vigna, B., 1981, Geometry and facies of small fault-controlled deep-sea fan systems in a transgressional depositional setting (Tertiary Piedmont Basin, north-western Italy): International Association of Sedimentologists, 2nd European Regional Meeting, Bologna, Excursions Guidebook, p. 5–56.

Cazzola, C., and Rigazio, G., 1983, Caratteri sedimentologici dei corpi torbiditici di Valla e Mioglia, Formazione di Rocchetta (Oligocene–Miocene) del Bacino Terziario Piemontese: Giornale di Geologia, v. 45, p. 87–100.

Civa, A., 2013, Stratigrafia fisica ed analisi di facies dei depositi deltizi e torbiditici della Formazione di Molare nell'area di Mioglia (Oligocene, settore occidentale del bacino terziario Piemontese) [MS Thesis]: University of Parma, 229 p.

Corney, R.K.T., Peakall, J., Parsons, D.R., Elliot, L., Amos, K.J., Best, J.L., and Ingham, D.B., 2006, The orientation of helical flow in curved channels: Sedimentology, v. 53, p. 249–257.

Cullen, T.M., Collier, R., Gawthorpe, R.L., Hodgson, D.M., and Barrett, B.J., 2019, Axial and transverse deep-water sediment supply to syn-rift fault terraces: insights from the West Xylokastro Fault Block, Gulf of Corinth, Greece: Basin Research, v. 32, p. 1105–1139.

Cunha, R.S., Tinterri, R., and Muzzi Magalhaes, P., 2017, Annot Sandstone in the Peïra Cava basin: an example of an asymmetric facies distribution in a confined turbidite system (SE France): Marine and Petroleum Geology, v. 87, p. 60–79.

Dal Cin, R., 1968, "Pebble clusters": their origin and utilization in the study of paleocurrents: Sedimentary Geology, v. 2, p. 233–241.

di Biase, D., and Mutti, E., 2002, The "proto-Adriatic basin, " *in* Mutti, E., Ricci Lucchi, F., and Roveri, M., eds., Revisiting Turbidites of the Marnoso–Arenacea Formation and their Basin-Margin Equivalents: Problems with Classic Models: European Association of Geoscientists and Engineers, 64th Conference and Exhibition, Florence, Italy, Excursion Guidebook, Part I, p. 1–4.

Dykstra, M., and Kneller, B.C., 2009, Lateral accretion in a deep-marine channel complex: implications for channelized flow processes in turbidity currents: Sedimentology, v. 56, p. 1411–1432.

Edwards, C., McQuaid, S., Easton, S., Scott, D., Couch, A., Evans, R., and Hart, S., 2017, Lateral accretion in a straight slope channel system: an example from the Forties Sandstone of the Huntington Field, UK central North Sea, *in* Bowan, M., and Levell, B., eds., Petroleum Geology of the NW Europe: 50 Years of Learning: 8th Petroleum Geology Conference, Proceedings, doi:10.1144/PGC8.33.

Elter, P., and Marroni, M., 1991, Le Unità Liguri dell'Appennino Settentrionale: sintesi dei dati e nuove interpretazioni: Memorie Descrittive Carta Geologica d'Italia, v. 46, p. 121–138.

Falletti, P., Gelati, R., and Rogledi, S., 1995, Oligo-Miocene evolution of Monferrato and Langhe, related to deep structures, *in* Polino, R., and Sacchi, R., eds., Atti del convegno "Rapporti Alpi-Appennino": Rome, Accademia Nazionale delle Scienze, detta dei Quaranta, v. 14, p. 1–20.

Fildani, A., Hubbard, S.M., Covault, J.A., Maier, K.L., Romans, B.W., Traer, M., and Rowland, J.C., 2013, Erosion at inception of deep-sea channels: Marine and Petroleum Geology, v. 41, p. 48–61.

Gamberi, F., and Marani, M., 2011, Geomorphology and sedimentary processes of a modern confined braided submarine channel belt (Stromboli Slope Valley, southeastern Tyrrhenian Sea): Journal of Sedimentary Research, v. 81, p. 686–701.

Gamberi, F., Rovere, M., Dykstra, M., Kane, I.A., and Kneller, B.C., 2013, Integrating modern seafloor and outcrop data in the analysis of slope channel architecture and fill: Marine and Petroleum Geology, v. 41, p. 83–103.

Gelati, R., and Gnaccolini, M., 2003, Genesis and evolution of the Langhe Basin, with emphasis on the latest Oligocene–earliest Miocene and Serravallian: Atti Ticinesi di Scienze della Terra, v. 44, p. 3–18.

Ghibaudo, G., Massari, F., and Chiambretti, I., 2014, Oligo-Miocene tectono-sedimentary evolution of the Langhe Sub-basin: from continental to basinal setting (Tertiary Piedmont Basin, Northwestern Italy): Journal of Mediterranean Earth Sciences, v. 6, p. 53–144.

Haughton, P.D.W., 2000, Evolving turbidite systems on a deforming basin floor, Tabernas, SE Spain: Sedimentology, v. 47, p. 497–518.

Hodgson, D.M., and Haughton, P.D.W., 2004, Impact of syndepositional faulting on gravity current behaviour and deep-water stratigraphy: Tabernas–Sorbas Basin, SE Spain, *in* Lomas, S.A., and Joseph, P., eds., Confined Turbidite Systems: Geological Society of London, Special Publication 222, p. 135–158.

Howlett, D.M., Gawthorpe, R.L., Ge, Z., Rotevatn, A., and Jackson, C.A.L., 2021, Turbidites, topography and tectonics: evolution of submarine channel–lobe systems in the salt-influenced Kwanza Basin, offshore Angola: Basin Research, v. 33, p. 1076–1110.

Hubbard, S.M., Covault, J.A., and Fildani, A., 2014, The stratigraphic expression of formative processes in channels [Abstract]: American Geophysical Union, Fall Meeting 2014, no. EP53E-04.

Hubbard, S.M., Jobe, Z.R., Romans, B.W., Covault, J.A., Sylvester, Z., and Fildani, A., 2020, The stratigraphic evolution of a submarine channel: linking seafloor dynamics to depositional products: Journal of Sedimentary Research, v. 90, p. 673–686.

Imran, J., Islam, M.A., Huang, H., Kassem, A., Dickerson, J., Pirmez, C., and Parker, G., 2007, Helical flow couplets in submarine gravity under-flows: Geology, v. 35, p. 659–662.

Janocko, M., 2011, Deep water sinuous channels: their development and architecture [Ph.D. Thesis]: University of Bergen, 106 p.

Janocko, M., Nemec, W., Henriksen, S., and Warchoł, M., 2013, The diversity of deep-water sinuous channel belts and slope valley-fill complexes: Marine and Petroleum Geology, v. 41, p. 7–34.

Kane., I.A. Catterall, V., McCaffrey, W.D., and Martinsen, O.J., 2010, Submarine channel response to intrabasinal tectonics: the influence of lateral tilt: American Association of Petroleum Geologists, Bulletin, v. 94, p. 189–219.

Kolla, V., Posamentier, H.W., and Wood, L.J., 2007, Deep-water and fluvial sinuous channels: characteristics, similarities and dissimilarities, and modes of formation: Marine and Petroleum Geology, v. 24, p. 388–405.

Labourdette, R., and Bez, M., 2010, Element migration in turbidite systems: random or systematic depositional processes?: American Association of Petroleum Geologists, Bulletin, v. 94, p. 345–368.

Laubscher, H.P., 1991, The arcs of western Alps today: Eclogae Geologicae Helvetiae, v. 84, p. 613–651.

Laubscher, H.P., Biella, G.C., Cassinis, R., Gelati, R., Lozej, A., Scarascia, S., and Tabacco, I., 1992, The collisional knot in Liguria: Geologische Rundschau, v. 81, p. 275–289.

Leeder, M.R., and Alexander, J., 1987, The origin and tectonic significance of asymmetrical meander belts: Sedimentology, v. 34, p. 217–226.

Lorenz, C.R., 1969, Contribution à l'étude stratigraphique de l'Oligocene et du Miocene inferieur des confins liguro-piemontais (Italie): Istituto di Geologia dell'Università di Genova, Atti, v. 6, p. 253–888.

Lowe, D.R., 1979, Sediment gravity flows: their classification and some problems of application to natural flows and deposits, *in* Doyle, L.J., and Pilkey, O.H., eds., Geology of Continental Slopes: SEPM, Special Publication 27, p. 75–82.

Lowe, D.R., 1982, Sediment gravity flows: depositional models with special reference to the deposits of high-density turbidity currents: Journal of Sedimentary Petrology, v. 52, p. 279–297.

Maier, K.L., Fildani, A., McHargue, T., Paull, C.K., Graham, S.A., and Caress, D.W., 2012, Deep-water punctuated channel migration: high-resolution subsurface data from the Lucia Channel System, offshore California: Journal of Sedimentary Research, v. 82, p. 1–8.

Maier, K.L., Fildani, A., McHargue, T., Paull, C.K., Graham, S.A., and Caress, D.W., 2013, Punctuated deep-water channel migration: high-resolution subsurface data from the Lucia Chica channel system, offshore California, U.S.A.—Reply: Journal of Sedimentary Research, v. 83, p. 93–95.

Maier, K.L., Roland, E.C., Walton, M.A.L., Conrad, J.E., Brothers, D.S., Dartnell, P., and Kluesner, J.W., 2018, The tectonically controlled San Gabriel Channel–lobe transition zone, Catalina Basin, Southern California Borderland: Journal of Sedimentary Research, v. 88, p. 942–959.

Maino, M., Decarlis, A., Felletti, F., and Seno, S., 2013, Tectono-sedimentary evolution of the Tertiary Piedmont Basin (NW Italy) within the Oligo-Miocene central Mediterranean geodynamics: Tectonics, v. 32, p. 593–619.

Major, J.J., and Iverson, M.R., 1999, Debris-flow deposition: effects of pore-fluid pressure and friction concentrated at flow margins: Geological Society of America, Bulletin, v. 111, p. 1424–1434.

Marr, J.G., Harff, P.A., Shanmugam, G., and Parker, G., 2001, Experiments on subaqueous sandy gravity flows: the role of clay and water content in flow dynamics and depositional structures: Geological Society of America, Bulletin, v. 113, p. 1377–1386.

Mayall, M., Jones, E., and Casey, M., 2006, Turbidite channel reservoirs: key elements in facies prediction and effective development: Marine and Petroleum Geology, v. 23, p. 821–841.

Middleton, G.V., and Hampton, M.A., 1973, Sediment gravity flows: mechanics of flow and deposition, *in* Middleton, G.V., and Bouma, A.H., eds., Turbidites and Deep-water Sedimentation: Society of Economic Paleontologists and Mineralogists, Pacific Section, Short Course Notes, p. 1–38.

Mohrig, D., and Marr, J.G., 2003, Constraining the efficiency of turbidity current generation from submarine debris flows and slides using laboratory experiments: Marine and Petroleum Geology, v. 20, p. 883–899.

Molli, G., Crispini, L., Malusà, M., Mosca, P., Piana, F., and Federico, L., 2010, Geology of the Western Alps–Northern Apennine junction area: a regional review: Journal of the Virtual Explorer, v. 36, p. 1–49.

Mutti, E., 1992, Turbidite Sandstones: Agip, Istituto di Geologia, Università di Parma, San Donato Milanese, 275 p.

Mutti, E., and Normark, W.R., 1987, Comparing examples of modern and ancient turbidite systems: problems and concepts, *in* Leggett, J.K., and Zuffa, G.G., eds., Marine Clastic Sedimentology: London, Graham and Trotman, p. 1–38.

Mutti, E., and Normark, W.R., 1991, An integrated approach to the study of turbidite systems, *in* Weimer, P., and Link, M.H., eds., Seismic Facies and Sedimentary Processes of Submarine Fans and Turbidite Systems: New York, Springer-Verlag, p. 75–106.

Mutti, E., and Tinterri, R., 2004, Cross-stratified sandstones and multiple beds: evidence of internal flow divergence in turbidity currents caused by submarine topography [Abstract]: American Association of Petroleum Geologists, Annual Meeting, Abstract Book, 4 p.

Mutti, E., Papani, L., di Biase, D., Davoli, G., Mora, S., Segadelli, S., and Tinterri, R., 1995, Il Bacino Terziario Epimesoalpino e le sue implicazioni nei rapporti tra Alpi ed Appennino: Memorie di Scienze Geologiche, v. 47, p. 217–244.

Mutti, E., Davoli, G., Tinterri, R., and Zavala, C., 1996, The importance of fluvio-deltaic systems dominated by catastrophic flooding in tectonically active basins: Memorie di Scienze Geologiche, v. 48, p. 233–291.

Mutti, E., Tinterri, R., Remacha, E., Mavilla, N., Angella, S., and Fava, L., 1999, An introduction to the analysis of ancient turbidite basins from an outcrop perspective: American Association of Petroleum Geologists, Continuing Education Course Note Series, v. 39, 93 p.

Mutti, E., di Biase, D., Fava, L., Mavilla, N., Sgavetti, M., and Tinterri, R., 2002, The Tertiary Piedmont Basin, *in* Mutti, E., Ricci Lucchi, F., and Roveri, M., eds., Revisiting Turbidites of the Marnoso–Arenacea Formation and their Basin-Margin Equivalents: Problems with Classic Models: European Association of Geoscientists and Engineers, 64th Conference and Exhibition, Florence, Italy, Excursion Guidebook, Part II, p. 1–25.

Mutti, E., Tinterri, R., Benevelli, G., di Biase, D., and Cavanna, G., 2003, Deltaic, mixed and turbidite sedimentation of ancient foreland basins: Marine and Petroleum Geology, v. 20, p. 733–755.

Mutti, E., Bernoulli, D., Ricci Lucchi, F., and Tinterri, R., 2009, Turbidites and turbidity currents from Alpine "flysch" to the exploration of continental margins: Sedimentology, v. 56, p. 267–318.

Normark, W.R., 1985, Local morphologic controls and effects of basin geometry on flow processes in deep marine basins, *in* Zuffa, G.G., ed., Provenance of Arenites: Dordrecht, Springer, p. 47–63.

Oluboyo, A.P., Gawthorpe, R.L., Bakke, K., and Hadler-Jacobsen, F., 2014, Salt tectonic controls on deep-water turbidite depositional systems: Miocene, southwestern lower Congo basin, offshore Angola: Basin Research, v. 26, p. 597–620.

Peakall, J., McCaffrey, B., and Kneller, B., 2000, A process model for the evolution, morphology, and architecture of sinuous submarine channels: Journal of Sedimentary Research, v. 70, p. 434–448.

Pickering, K.T., and Hiscott, R.N., 2016, Deep Marine Systems: Processes, Deposits, Environments, Tectonics and Sedimentation, First Edition: American Geophysical Union, 637 p.

Pickering, K.T., Hodgson, D.M., Platzman, E., Clark, J.D., and Steffens, C., 2001, A new type of bedform produced by backfilling processes in a submarine channel, late Miocene, Tabernas–Sorbas basin, SE Spain: Journal of Sedimentary Research, v. 71, p. 692–704.

Pirmez, C., and Imran, J., 2003, Reconstruction of turbidity currents in Amazon Channel: Marine and Petroleum Geology, v. 20, p. 823–849.

Prather, B.E., Booth, J.R., Steffens, G.S., and Craig, P.A., 1998, Classification, lithologic calibration, and stratigraphic succession of seismic facies of intraslope basins, deep-water Gulf of Mexico: American Association of Petroleum Geologists, Bulletin, v. 82, p. 701–728.

Remacha, E., Fernandez, L.P., Maestro, E., Oms, O., Estrada, R., and Teixell, A., 1998, The upper Hecho Group turbidites and their vertical evolution to deltas (Eocene south-central Pyrenees), *in* Melendez Hevia, A., and Soria, A.R., eds., 15th International Sedimentological Congress, Excursion Guidebook, complementary information, 21 p.

Remacha, E., Fernandez, L.P., and Maestro, E., 2005, The transition between sheet-like lobe and basin plain turbidites in the Hecho basin (south-central Pyrenees, Spain): Journal of Sedimentary Research, v. 75, p. 789–819.

Rossi, M., and Craig, J., 2016, A new perspective on sequence stratigraphy of syn-orogenic basins: insights from the Tertiary Piedmont Basin (Italy) and implications for play concepts and reservoir heterogeneity, *in* Bowman, M., Smyth, H.R., Good, T.R., Passey, S.R., Hirst, J.P.P., and Jordan, C.J., eds., The Value of Outcrop Studies in Reducing Subsurface Uncertainty and Risk in Hydrocarbon Exploration and Production: Geological Society of London, Special Publication 436, p. 93–133.

Rossi, M., Mosca, P., Rogledi, S., Polino, R., and Biffi, U., 2009, New outcrop and subsurface data in the Tertiary Piedmont Basin (NW-Italy): unconformity-bounded stratigraphic units and their relationships with basin-modification phases: Rivista Italiana di Paleontologia e Stratigrafia, v. 115, p. 305–335.

Sanders, J.E., 1965, Primary sedimentary structures formed by turbidity currents and related resedimentation mechanisms, *in* Middleton, G.V., ed., Primary Sedimentary Structures and Their Hydrodynamic Interpretation: SEPM, Special Publication 12, p. 192–219.

Schumm, S.A., Dumont, J.F., and Holbrook, J.M., 2000, Active Tectonics and Alluvial Rivers: Cambridge, Cambridge University Press, 276 p.

Shanmugam, G., 1996, High-density turbidity currents: Are they sandy debris flows?: Journal of Sedimentary Research, v. 66, p. 2–10.

Smith, G., Rowley, P., Williams, R., Giordano, G., Trolese, M., Silleni, A., Parsons, D.R., and Capon, S., 2020, A bedform phase diagram for dense granular currents: Nature Communications, v. 11, p. 1–11.

Sohn, Y.K., Rhee, C.W., and Kim, B.C., 1999, Debris flow and hyperconcentrated flood-flow deposits in an alluvial fan, north-western part of the Cretaceous Yongdong Basin, Central Korea: Journal of Geology, v. 107, p. 111–132.

Sohn, Y.K., Choe, M.Y., and Jo, H.R., 2002, Transition from debris flow to hyperconcentrated flow in a submarine channel (the cretaceous Cerro Toro Formation, southern Chile): Terra Nova, v. 14, p. 405–415.

Soutter, E.L., Bell, D., Cumberpatch, Z.A., Ferguson, R.A., Spychala, Y.T., Kane, I.A., and Eggenhuisen, J.T., 2021, The influence of confining topography orientation on experimental turbidity currents and geological implications: Frontiers in Earth Sciences, v. 8, 540633.

Sumner, E.J., Peakall, J., Dorrell, R.M., Parsons, D.R., Darby, S.E., Wynn, R.B., and White, D., 2014, Driven around the bend: spatial evolution and controls on the orientation of helical bend flow in a natural submarine gravity current: Journal of Geophysical Research: Oceans, v. 119, p. 898–913.

Tagliaferri, A., and Tinterri, R., 2016, The tectonically confined Firenzuola turbidite system (Marnoso–Arenacea Formation, northern Apennines, Italy): Italian Journal of Geosciences, v. 135, p. 425–443.

Tagliaferri, A., Tinterri, R., Pontiggia, M., Da Pra, A., Davoli, G., and Bonamini, E., 2018, Basin-scale, high-resolution three-dimensional facies modeling of tectonically confined turbidites: an example from the Firenzuola system (Marnoso–Arenacea Formation, northern Apennines, Italy): American Association of Petroleum Geologists, Bulletin, v. 102, p. 1601–1626.

Tinterri, R., 1994, Sedimentologia e stratigrafia della Formazione di Molare nella regione di Mioglia (SV) (settore occidentale del Bacino Terziario Piemontese) [MS Thesis]: University of Parma, 115 p.

Tinterri, R., and Civa, A., 2014, Lateral accretions in low efficiency turbidites associated with a structurally-induced topography (Oligocene Molare Unit, Tertiary Piedmont basin, north-western Italy): 19th International Sedimentological Congress, Geneva, p. 689.

Tinterri, R., and Muzzi Magalhaes, P., 2011, Synsedimentary structural control on foredeep turbidites: an example from Miocene Marnoso–Arenacea Formation, Northern Apennines, Italy: Marine and Petroleum Geology, v. 28, p. 629–657.

Tinterri, R., and Piazza, A., 2019, Turbidites facies response to the morphological confinement of a foredeep (Cervarola Sandstones Formation, Miocene, northern Apennines, Italy): Sedimentology, v. 66, p. 636–674.

Tinterri, R., and Tagliaferri, A., 2015, The syntectonic evolution of foredeep turbidites related to basin segmentation: facies response to the increase in tectonic confinement (Marnoso–Arenacea Formation, Miocene, Northern Apennines, Italy): Marine and Petroleum Geology, v. 67, p. 81–110.

Tinterri, R., Drago, M., Consonni, A., Davoli, G., and Mutti, E., 2003, Modelling subaqueous bipartite sediment gravity flows on the basis of outcrop constraints: first results: Marine and Petroleum Geology, v. 20, p. 911–933.

Tinterri, R., Muzzi Magalhaes, P., Tagliaferri, A., and Cunha, R.S., 2016, Convolute laminations and load structures in turbidites as indicators of flow reflections and decelerations against bounding slopes. Examples from the Marnoso–Arenacea Formation (northern Italy) and Annot Sandstones (south eastern France): Sedimentary Geology, v. 344, p. 382–407.

Tinterri, R., Laporta, M., and Ogata, K., 2017, Asymmetrical cross-current turbidite facies tract in a structurally-confined mini-basin (Priabonian–Rupelian, Ranzano Sandstone, northern Apennines, Italy): Sedimentary Geology, v. 352, p. 63–87.

Tinterri, R., Civa, A., Laporta, M., and Piazza, A.L., 2020, Turbidites and turbidity currents, *in* Scarselli, N., Jürgen, A., Chiarella, D., Roberts, D.G., and Bally, A.W., eds., Regional Geology and Tectonics: Principles of Geologic Analysis, 2nd Edition, Elsevier, p. 441–479.

Wynn, R.B., Cronin, B.T., and Peakall, J., 2007, Sinuous deep-water channels: genesis, geometry and architecture: Marine and Petroleum Geology, v. 24, p. 341–387.

Received 6 November 2020; accepted 13 March 2021.